Cell Reports
Medicine

Article

Unified framework for patient-derived, tumor-organoid-based predictive testing of standard-of-care therapies in metastatic colorectal cancer

Graphical abstract

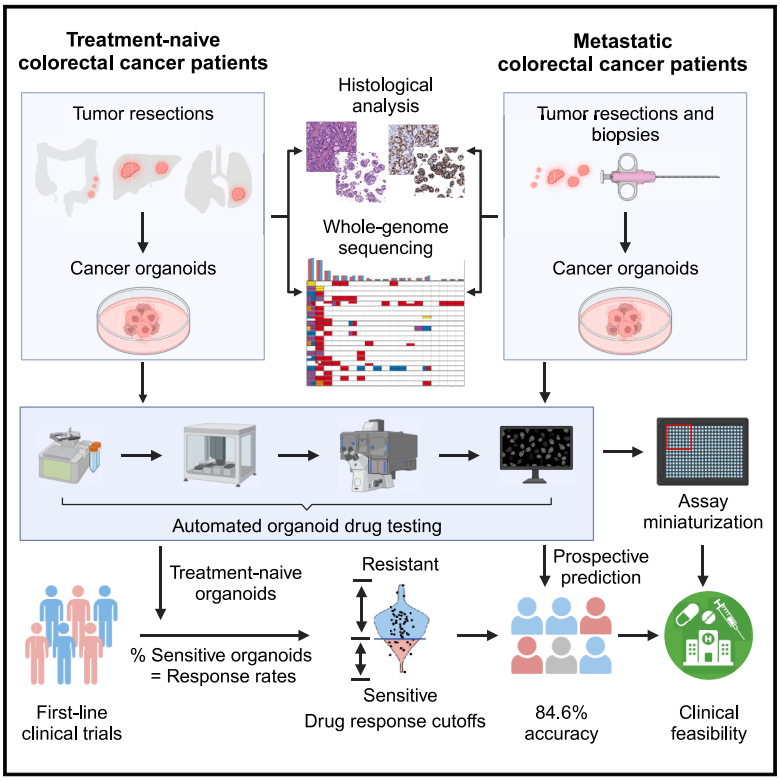

Highlights

- PDTO routine drug testing framework for mCRC based on clinical trial response rates
- PDTO drug testing shows 85% accuracy and association with progression-free survival
- Liver is the optimal metastatic site for biopsy sampling for PDTO generation
- Clinical reporting within a 7-week time frame is feasible with assay miniaturization

Authors

Tao Tan, Dmitri Mouradov, Margaret Lee, ..., Antony W. Burgess, Peter Gibbs, Oliver M. Sieber

Correspondence

sieber.o@wehi.edu.au

In brief

Tan et al. describe a framework for predictive tumor-organoid-based testing of standard-of-care therapies for patients with metastatic colorectal cancer, demonstrating assay accuracy and feasibility of clinical reporting. Predictive organoid drug testing can complement routine genomic marker analyses, facilitating selection of the most active agents and avoidance of ineffective treatments.

Tan et al., 2023, Cell Reports Medicine *4*, 101335
December 19, 2023 © 2023 The Author(s).
https://doi.org/10.1016/j.xcrm.2023.101335

CellPress

Cell Reports Medicine

CellPress
OPEN ACCESS

Article

Unified framework for patient-derived, tumor-organoid-based predictive testing of standard-of-care therapies in metastatic colorectal cancer

Tao Tan,[1,2,13] Dmitri Mouradov,[1,2,13] Margaret Lee,[1,3,4,5,13] Grace Gard,[1,3,13] Yumiko Hirokawa,[1] Shan Li,[1] Cong Lin,[6,7] Fuqiang Li,[6,7] Huijuan Luo,[6,7] Kui Wu,[6,7] Michelle Palmieri,[1,2] Evelyn Leong,[1] Jordan Clarke,[1] Anuratha Sakthianandeswaren,[1,2] Helen Brasier,[1] Jeanne Tie,[1,2,3] Niall C. Tebbutt,[8] Azim Jalali,[1,3,9,10] Rachel Wong,[4,5] Antony W. Burgess,[1,2,11] Peter Gibbs,[1,2,3] and Oliver M. Sieber[1,2,11,12,14,*]

[1]Personalised Oncology Division, The Walter and Eliza Hall Institute of Medical Research, Parkville, VIC 3052, Australia
[2]Department of Medical Biology, The University of Melbourne, Parkville, VIC 3052, Australia
[3]Department of Medical Oncology, Western Health, Footscray, VIC 3011, Australia
[4]Department of Medical Oncology, Eastern Health, Box Hill, VIC 3128, Australia
[5]Eastern Health Clinical School, Faculty of Medicine, Nursing, and Health Sciences, Monash University, Box Hill, VIC 3128, Australia
[6]HIM-BGI Omics Center, Zhejiang Cancer Hospital, Hangzhou Institute of Medicine, Chinese Academy of Sciences, BGI Research, Hangzhou 310000, China
[7]Guangdong Provincial Key Laboratory of Human Disease Genomics, Shenzhen Key Laboratory of Genomics, BGI Research, Shenzhen 518083, China
[8]Department of Medical Oncology, Olivia Newton-John Cancer Wellness & Research Centre, Austin Health, Heidelberg, VIC 3084, Australia
[9]Department of Cancer Services, Latrobe Regional Hospital, Traralogon, VIC 3844, Australia
[10]Department of Medical Oncology, The Northern Hospital, Epping, VIC 3076, Australia
[11]Department of Surgery, The University of Melbourne, Parkville, VIC 3050, Australia
[12]Department of Biochemistry and Molecular Biology, Monash University, Clayton, VIC 3800, Australia
[13]These authors contributed equally
[14]Lead contact
*Correspondence: sieber.o@wehi.edu.au
https://doi.org/10.1016/j.xcrm.2023.101335

SUMMARY

Predictive drug testing of patient-derived tumor organoids (PDTOs) holds promise for personalizing treatment of metastatic colorectal cancer (mCRC), but prospective data are limited to chemotherapy regimens with conflicting results. We describe a unified framework for PDTO-based predictive testing across standard-of-care chemotherapy and biologic and targeted therapy options. In an Australian community cohort, PDTO predictions based on treatment-naive patients (n = 56) and response rates from first-line mCRC clinical trials achieve 83% accuracy for forecasting responses in patients receiving palliative treatments (18 patients, 29 treatments). Similar assay accuracy is achieved in a prospective study of third-line or later mCRC treatment, AGITG FORECAST-1 (n = 30 patients). "Resistant" predictions are associated with inferior progression-free survival; misclassification rates are similar by regimen. Liver metastases are the optimal site for sampling, with testing achievable within 7 weeks for 68.8% cases. Our findings indicate that PDTO drug panel testing can provide predictive information for multifarious standard-of-care therapies for mCRC.

INTRODUCTION

Metastatic colorectal cancer (mCRC) remains the second leading cause of cancer-related mortality worldwide despite increasing therapy options.[1] Heterogeneous treatment responses remain a principal challenge to improving outcomes, with limited clinical means to predict treatment efficacy. Precision oncology for directing therapy use is routinely limited to *RAS* (*KRAS* and *NRAS*) mutation status for anti-EGFR antibody therapy, DNA mismatch repair (dMMR) status (microsatellite instability-high [MSI-H]/dMMR) for immunotherapy, and more recently $BRAF^{V600E}$ mutation status for BRAF-targeted therapies and HER2/ERBB2 amplification status for HER2-targeted therapies.[2–10] For most treatments, there are no markers to predict responses, and even for genomically selected patients, response rates are often low. Consequently, many patients receive ineffective, costly drugs and suffer unnecessary toxicities.

A promising *ex vivo* approach to predict treatment benefit is personalized tumor response testing using patient-derived tumor organoids (PDTOs).[11] PDTOs are self-organizing three-dimensional structures that can be readily derived from fresh patient tumor specimens, mirror the histologic and genomic features of the original tumor, and are eminently suitable for high-throughput drug testing.[12–17]

This is an open access article under the CC BY-NC-ND license (http://creativecommons.org/licenses/by-nc-nd/4.0/).

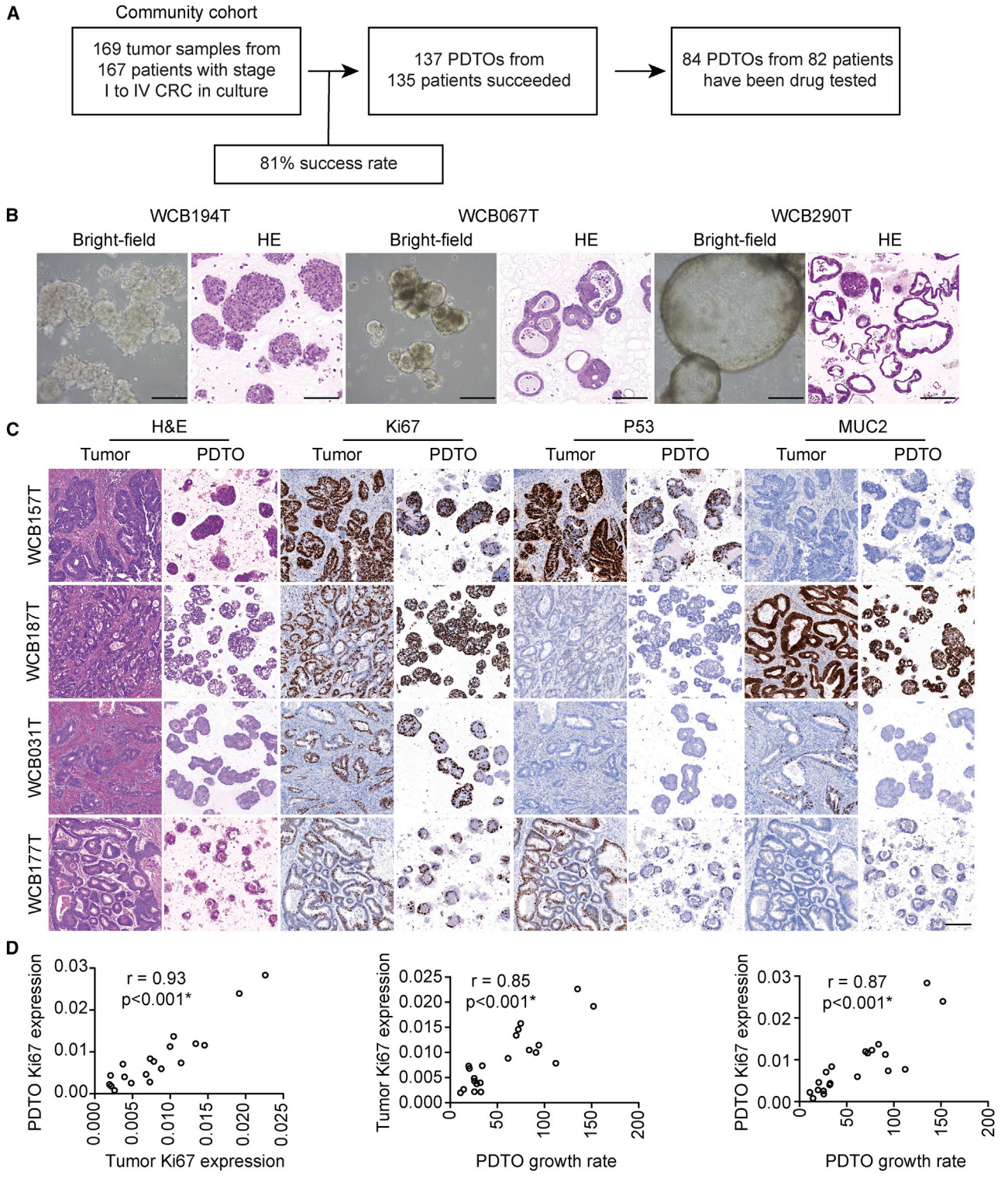

Figure 1. PDTO generation and histopathologic validation for patients with stage I–IV CRC enrolled in the ACCORD-CRC and TRACC registries

(A) Flow chart indicating the number of patients with stage I–IV CRC included, the success rate of establishing cultures from patients, and the number of PDTO lines progressed to drug sensitivity testing.

(legend continued on next page)

Post hoc studies for multiple cancer types indicate that PDTO response can emulate the therapeutic response of the matched patient.[12–14,18–21] However, few prospective studies have attempted to define classification standards for PDTO assay predictions,[13,14] and fewer still have validated predictive PDTO assays in independent patient cohorts.[21,22]

Currently, two prospective observational studies have reported on PDTO assay accuracies for mCRC treatment. The single-cohort TUMOROID study, fitting prediction cutoffs based on Response Evaluation Criteria in Solid Tumors (RECIST) response of the metastatic lesion from which the PDTO was derived, achieved an accuracy of 86.4% for irinotecan-based, second-line treatment but found poor performance for first-line treatment with 5-fluorouracil plus oxaliplatin (FOLFOX).[13] Wang et al., defining a joint prediction cutoff for FOLFOX and 5-fluorouracil (5FU) plus irinotecan (FOLFIRI) neoadjuvant or adjuvant chemotherapy based on best RECIST response, American Joint Committee on Cancer/College of American Pathologists (AJCC/CAP) regression grade, or carcinoembryonic antigen (CEA) levels, achieved a 79.7% accuracy in an independent validation cohort, although data were not detailed by treatment setting or regimen.[21]

While previous prospective studies have focused on 5FU-, oxaliplatin-, and irinotecan-based chemotherapies, PDTO predictive assays encompassing the spectrum of available standard-of-care chemotherapy and biologic and targeted therapy options remain to be explored. Moreover, while previous studies indicate that PDTO assay turnaround times for small numbers of treatments in defined clinical scenarios are achievable with time frames for patient management,[12–14,21] whether this can be realized for routine panel testing of standard-of-care therapeutics is uncertain. Other challenges to diagnostic translation include success rate of PDTO generation from biopsy samples, assay standardization, and automation and processes for clinical reporting.

Here, we embarked on establishing a unified framework for PDTO standard-of-care drug testing and clinical reporting. To develop a PDTO assay applicable across mainstay therapies compatible with PDTO monoculture (5FU, oxaliplatin, irinotecan, FOLFOX, FOLFIRI, trifluridine/tipiracil, regorafenib, and anti-EGFR antibodies), we prospectively implemented a standardized robotic assay platform in a multicenter CRC community cohort where treatment and outcome data were prospectively collected in a clinical registry. Therapy-specific cutoff values for PDTO assay predictions were derived based on treatment-naive patients with CRC and response rates from first-line mCRC clinical trials, with evaluation of predictive accuracy in independent patients with mCRC receiving palliative treatment. We then conducted a prospective multicenter, observational clinical study to evaluate our PDTO drug testing framework in the third-line or later mCRC treatment setting (FORECAST-1, sponsored by AGITG, ACTRN12620001353987). Primary study aims were determination of clinical feasibility of PDTO drug panel testing and development of a process for clinical reporting, including validation of PDTO assay accuracy and assessment of success rate and turnaround time.

RESULTS

Initial community cohort implementation of a standardized PDTO drug testing platform

Prospective collection of tumor tissues from patients with newly diagnosed or recurrent CRC for PDTO generation was implemented across four hospitals in Melbourne, Australia, with standardized capture of treatment and outcome data (community cohort, Figure 1A).[23,24] A total of 169 CRC tissue samples were obtained from 167 patients with CRC at resection of primary tumor (21 stage I, 56 stage II, 54 stage III, and 18 stage IV) or metastatic disease (n = 20), including one patient with primary tumor and liver metastasis and one patient with liver and lung metastasis samples. Patient characteristics are shown in Table S1.

PDTOs were grown in low-viscosity matrix (LVM) suspension culture medium to facilitate passaging and dispensing as described previously[25]; Wnt ligands were omitted to prevent the outgrowth of normal colorectal epithelium. Overall, 81.1% (137 of 169) PDTO LVM cultures were successfully established and biobanked, with similar establishment rates by patient sex, age at diagnosis, tumor stage, primary tumor site, grade, and *RAS* status but lower success rates for stage II, MMR-deficient, and *RAF* mutant tumors (Table S1). PDTO lines exhibited heterogeneous morphologies ranging from predominantly compact to cystic structures (Figure 1B).

PDTOs grown in LVM culture conditions were confirmed to resemble the histologic and genomic features of the original tumor. Marker expression analysis demonstrated similar staining patterns for Ki67, p53, and Muc2 (Figure 1C), with proportions of Ki67-positive cells further correlating with PDTO growth rates as determined by time-lapse imaging (Figure 1D).[25] Whole-genome sequencing (WGS) of PDTOs at a median passage of 7 (range 1–22) and matched tumor and germline DNA from 21 patients demonstrated similar total mutation loads and point mutation types, including for two hypermutated cases with dMMR deficiency (WCB046) and DNA polymerase epsilon (POLE) mutation (WCB268) (Figure 2A). Genome-wide somatic single-nucleotide variant (SNV) analysis revealed a median SNV overlap of 72.2% (range, 49.4%–87.8%) between PDTO and matched tumor samples (Figure 2A), with analysis of the mutational spectrum in the most frequently mutated CRC genes showing a median overlap of 97.5% (range 81.0%–100%) (Figure 2B). PDTOs also recapitulated the genome-wide DNA copy-number variation (CNV) patterns of paired tumors (Figure 2C), with both showing frequent deletions of chromosome arms 8p, 17p (including *TP53*), and 18q (including *SMAD4*) and gains of chromosomes

(B) Representative bright-field images and H&E-stained sections of PDTOs grown in LVM suspension culture medium illustrating heterogeneous morphologies ranging from solid/compact structures to thin-walled cystic structures. Scale bars, 200 μm.
(C) Representative H&E staining and immunohistochemistry results for PDTOs from patients stained for Ki67, p53, and MUC2. Scale bars, 200 μm.
(D) Correlation of tumor Ki67 expression and PDTO Ki67 expression, PDTO growth rate and tumor Ki67 expression, and PDTO growth rate and PDTO Ki67 expression (n = 21 tissues and n = 20 PDTOs). Statistical significance was attributed to values of $p < 0.050$ as determined by the correlation test. *$p < 0.050$.
See also Table S1.

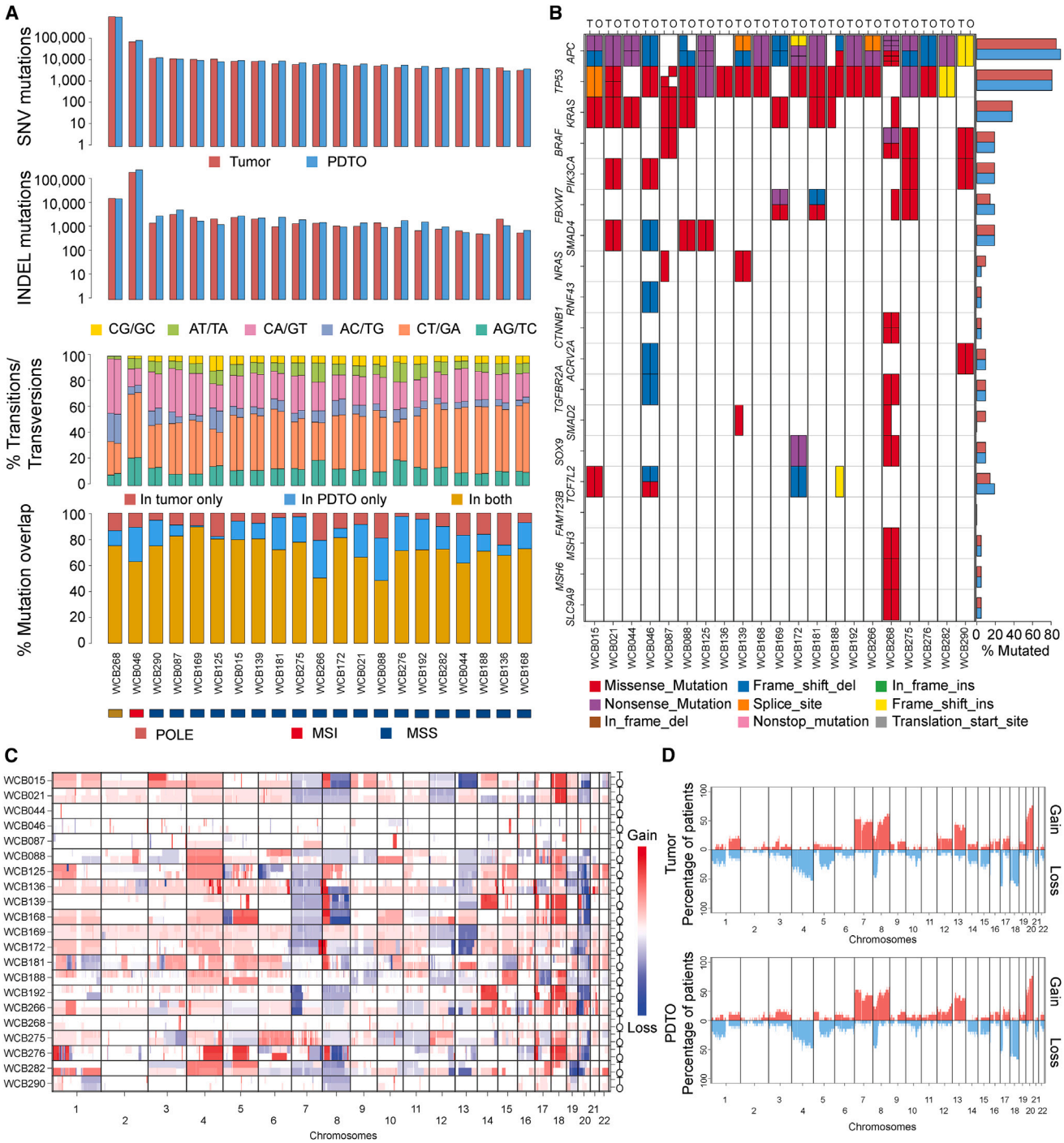

Figure 2. Genomic features of PDTOs and matched original tumor tissues from the community cohort as determined by whole-genome sequencing

(A) Mutation profiles of 21 PDTOs and matched tumor tissues, including counts of SNVs and insertions or deletions (indels), proportions of nucleotide transitions and transversions, and overlap for genome-wide somatic SNVs.

(B–D) Somatic mutation spectra for the most frequently mutated CRC genes (B), genome-wide relative DNA copy-number aberrations (C), and frequencies of DNA copy-number gains and losses for PDTOs and matched tumor tissues (D). T, tumor; O, patient-derived tumor organoid.

See also Table S2.

7, 8q (including *MYC*), 13, and 20q (Figure 2D). Assessment of matched PDTO and tumor samples for systematic differences in genomic alterations identified no recurrent changes in >2 sample pairs for gene mutations and no bias in gene copy-number gain or loss (Table S2). There was no relationship between PDTO passage number and mutation burden for non-hypermutated cases ($r = 0.11$; $p = 0.667$; correlation test).

84 PDTO lines from 82 patients with available treatment and follow-up data were progressed to drug sensitivity testing on a previously validated high-throughput imaging platform in a central laboratory (Figure 3A; Table S1).[25] PDTOs were exposed to standard-of-care single-agent and combination therapies compatible with PDTO monoculture (5FU, oxaliplatin, SN38 [active metabolite of irinotecan], regorafenib, TAS-102 [trifluridine/tipiracil], FOLFOX, and FOLFIRI), and clinically accessible agents with reported activity in single-arm phase 2 studies (gemcitabine,[26,27] pemetrexed,[28–30] and temozolomide[31]). Erlotinib was used as a surrogate for anti-EGFR antibodies, as the latter required a different vehicle from the other compounds. Single agents were assayed in duplicate in 9-step, 4-fold dilution series; FOLFOX and FOLFIRI treatments were assayed in duplicate in 7 × 7 drug matrices of 5FU and oxaliplatin or SN38, respectively, with 4-fold dilution series of treatment components. Standard-of-care drug titration ranges encompassed patient-relevant drug concentrations (5FU [$C_{max} \approx 7.5$ μM][32]; oxaliplatin [$C_{max} \approx 5.0$ μM][33]; SN38 [$C_{max} \approx 0.14$ μM][33]; regorafenib [$C_{max} \approx 7.3$ μM] [ClinicalTrials.gov: NCT01853046]; TAS-102 [$C_{max} \approx 18.2$ μM] [AusPAR 2018]; and erlotinib [$C_{max} \approx 4.6$ μM] [ClinicalTrials.gov: NCT00965731]); highest concentrations for investigational agents were 15 μM for gemcitabine, 10 μM for pemetrexed, and 750 μM for temozolomide. PDTOs were grown from single cells over a 3-day period followed by compound addition from preprepared drug dilution plates. PDTOs were then imaged daily for 7 days for PDTO-size-based quantification of viability as validated previously (Figures 3B and 3C).[25] Raw and processed PDTO viability data for the community cohort are provided in Tables S3 and S4. Drug responses were quantified as area under the dose-response curve (AUC) for single agents and as mean "pan-matrix" viability score for drug combinations.

Coefficients of variation (CVs) for vehicle control wells were less than 20% for all assay plates (n = 168), and PDTOs screened on two separate occasions showed concordant results (Figures S1A and S1B). As anticipated, drug sensitivity profiles varied considerably between individual PDTOs for all single-agent and combination treatments (Figure 3D). Erlotinib sensitivity correlated with cetuximab sensitivity and showed the expected association with *RAS* mutation status, with resistance demonstrated in RAS^{Mut} PDTOs (Figures 3E and 3F). For the two patients with PDTOs available from two different lesions, drug testing results showed strong correlations (primary tumor and liver metastasis: $r = 0.89$; $p = 0.0013$; liver and lung metastases: $r = 0.70$; $p = 0.036$, correlation test).

PDTO-based prediction model for standard-of-care drug testing in mCRC

To develop a predictive PDTO assay applicable across standard-of-care therapy options for mCRC, we defined therapy-specific cutoff values based on drug sensitivity profiles of treatment-naive patients from our initial community cohort (n = 56) and response rates reported in clinical trials of first-line therapy (Figure 4A): 25% for 5FU and TAS-102, 20% for irinotecan, oxaliplatin, and anti-EGFR antibody therapy (for RAS^{WT} tumors), 10% for regorafenib, and 50% for FOLFIRI and FOLFOX (clinical trial details in Table S5). Prediction cutoff values were applied to community patients treated for metastatic disease post-PDTO generation (18 patients, 29 evaluable treatments). One patient had received neoadjuvant treatment for a primary rectal cancer; however, the PDTO for this patient was derived from a recurrent liver metastasis. *In vitro* drug response predictions were correlated with clinical outcomes, defining patients with complete response (CR), partial response (PR), or stable disease (SD) for more than 24 weeks by clinician assessment as experiencing clinical benefit. For patients receiving both chemotherapy and biologic therapy in a line of treatment, PDTOs were considered "sensitive" if sensitivity was observed to at least one treatment component; similarly, response to FOLFOXIRI therapy was scored based on both FOLFOX and FOLFIRI matrices.

PDTO-based drug response predictions were highly correlated with patient clinical outcomes with concordance for 24 of 29 treatments (Figure 4B). Among 11 treatments with matched PDTOs predicting sensitivity, 10 were associated with clinical benefit, and 1 was not; among 18 treatments with PDTOs predicting resistance, 14 did not result in clinical benefit, and 4 did. Thus, classification achieved an accuracy of 82.8% (95% confidence interval [CI] = 64.2%–94.2%) with 71.4% sensitivity (true positive rate) and 93.3% specificity (true negative rate) ($p < 0.0005$ for accuracy (Acc) > non-informative rate (NIR); binomial test). The median time from PDTO harvest to treatment was 9 weeks (range, 2–53 weeks), with no association between this time window and assay accuracy ($p = 0.766$; Student's t test).

Feasibility of organoid response assessment to define effective treatments for patients with CRC after failure of standard therapy (AGITG FORECAST-1)

To evaluate clinical feasibility of PDTO drug panel testing for patients with mCRC and develop a process for clinical reporting of PDTO results, taking into account other relevant clinical information, we conducted a prospective, multicenter observational study in the third-line or later mCRC treatment setting (AGITG FORECAST-1). Between September 2020 and December 2021, 30 patients were enrolled, with a median age of 59 years (range, 36–71). Fresh tumor biopsies were obtained from liver (n = 16), peritoneum (n = 6), lung (n = 3), lymph node (n = 2), primary tumor (n = 1), brain (n = 1), and bone (n = 1). Patient characteristics are shown in Table S6.

Overall, we achieved a 63.3% (19 of 30) success rate of PDTO establishment and drug sensitivity testing from biopsy specimens (Figure 5A). Six tissue cultures did not form PDTOs, and five PDTO cultures failed to expand. Examination of culture success rates by site of biopsy sampling identified CRC liver metastases as the optimal location, achieving a 75.0% (12 of 16) success rate as compared to 50.0% (7 of 14) for metastases from other sites. For all assay plates, CVs for vehicle control wells were less than 20% (Figure S1C). Time from PDTO biopsy to drug screen result for our 9 single-agent and 2 combination treatments based on

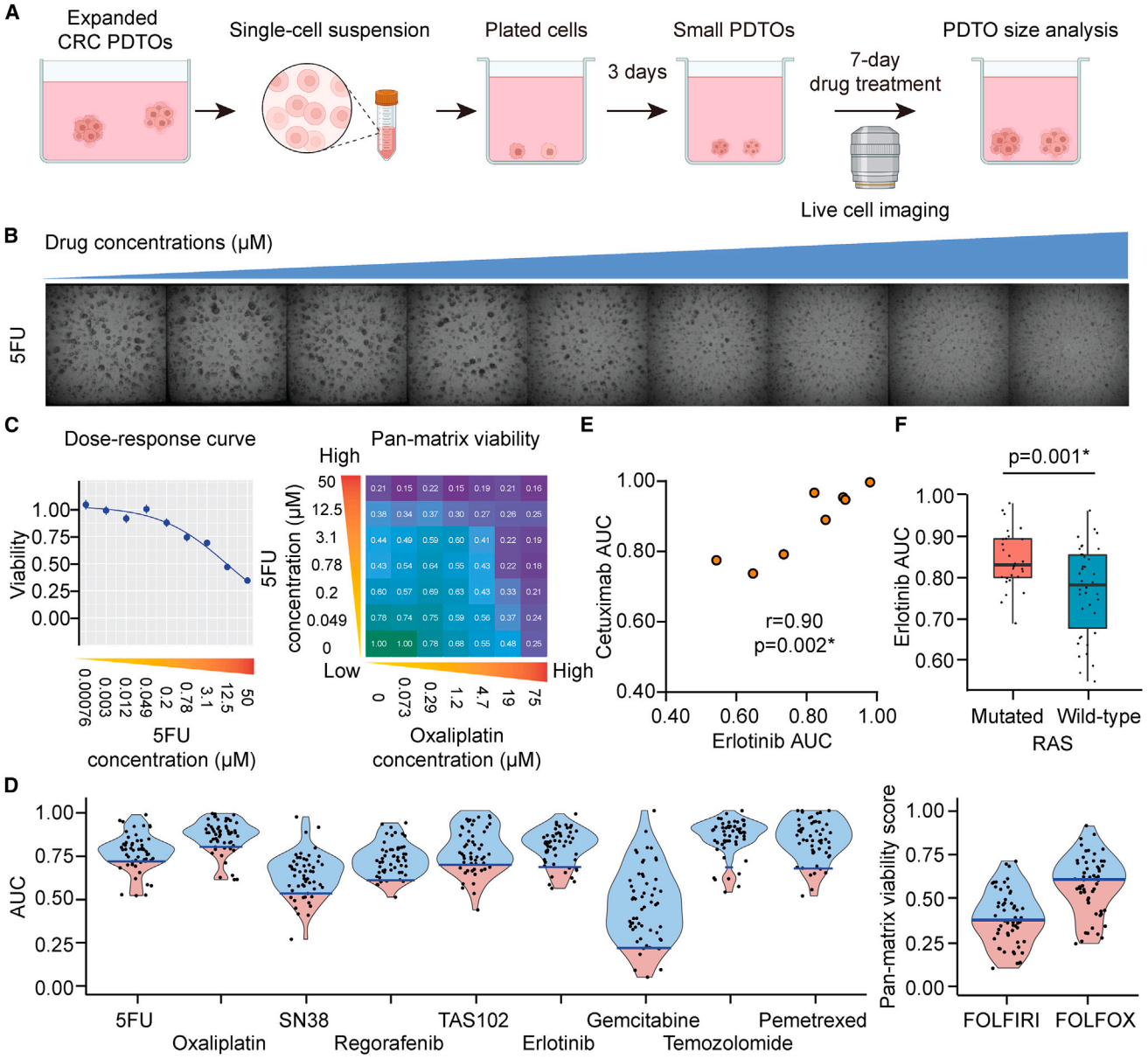

Figure 3. PDTO drug sensitivity for patients with stage I–IV CRC enrolled in the ACCORD-CRC and TRACC registries

(A) Schematic of the standardized workflow for semiautomated PDTO drug testing. Established tumoroids were dissociated and seeded as single cells, grown into small PDTOs over 3 days, and treated with drug for 7 days with daily bright-field imaging; viability was quantified by determination of mean PDTO size.

(B) Representative images of PDTOs treated with increasing 5FU concentrations on day 10 of the assay.

(C) Representative PDTO dose-response curve for 5FU single-agent treatment and viability matrix for 5FU-oxaliplatin combination treatment.

(D) Drug sensitivity profiles for 56 PDTO lines from 56 chemo-naive patients with CRC for single-agent 5FU, oxaliplatin, SN38, regorafenib, TAS-102, erlotinib, gemcitabine, pemetrexed, and temozolomide treatments and combination 5FU-oxaliplatin and 5FU-SN38 treatments; indicated cutoffs are based on treatment-naive patients and response rates from clinical trials of first-line mCRC treatment; blue, resistant; red, sensitive.

(E) Correlation of PDTO erlotinib versus cetuximab sensitivity (n = 8 PDTOs). Statistical significance was attributed to values of $p < 0.050$ as determined by the correlation test.

(F) Comparison of erlotinib sensitivity between RAS^{Mut} (n = 28) and RAS^{WT} (n = 38) PDTOs. Statistical significance was attributed to values of $p < 0.050$ as determined by the Student's t test. *$p < 0.050$.

See also Figures S1 and S5 and Tables S1, S3, and S4.

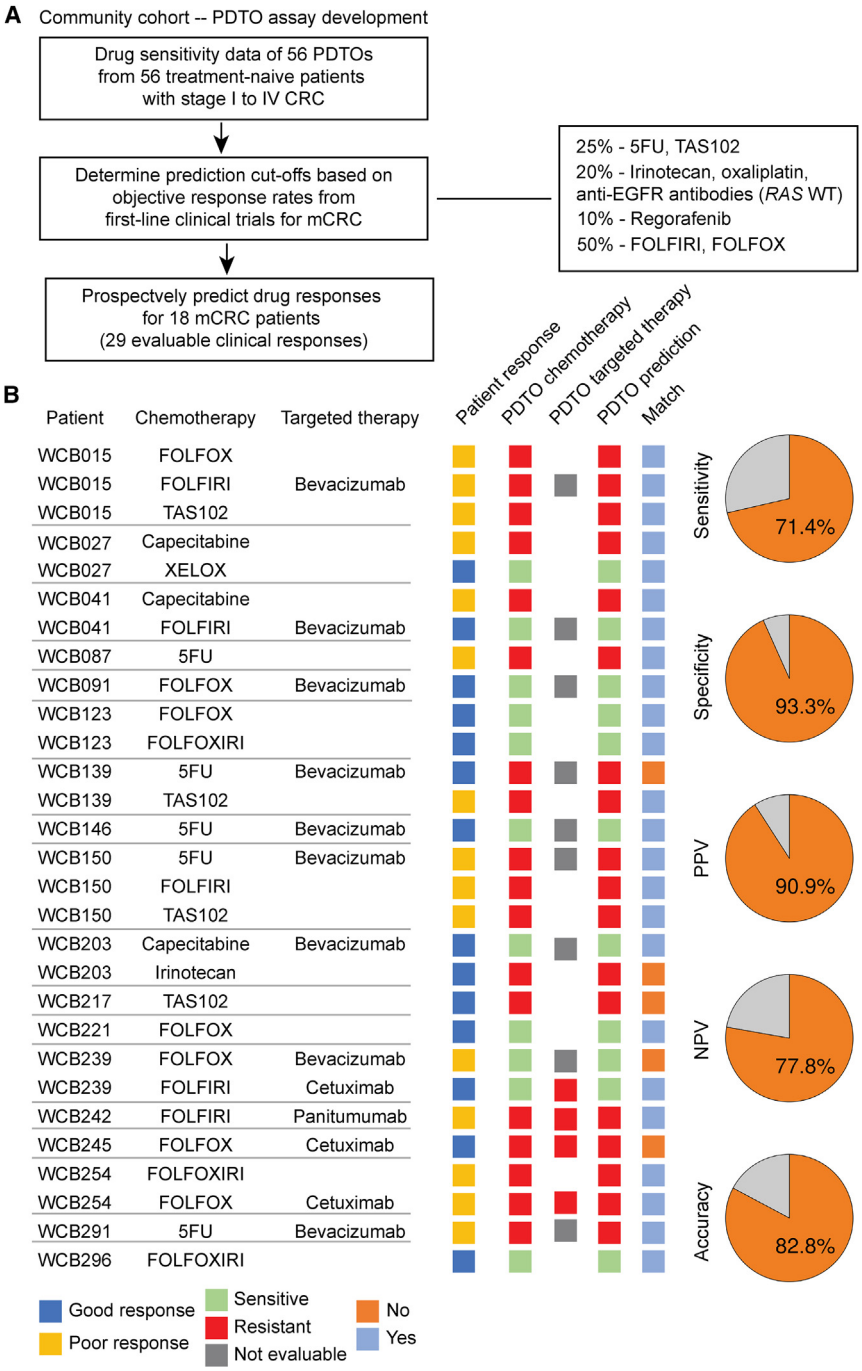

Figure 4. PDTO-based prediction model for standard-of-care drug testing in mCRC

(A) Flow chart indicating the number of PDTOs from treatment-naive community patients and response rate cutoffs from first-line mCRC clinical trials used for predictive model development and the number of PDTOs from an independent validation cohort of community patients used for prospective model evaluation.

(B) Details of mCRC patient treatments, clinical outcomes, PDTO predictions, and matching status of predictions and responses (18 patients, 29 treatments). Pie charts detail model accuracy, sensitivity, specificity, positive predictive value (PPV), and negative predictive value (NPV).

See also Table S5.

duplicate 9-step dose-response curves and 7 × 7 drug matrices ranged from 25 to 144 days (median, 72 days). Raw and processed PDTO viability data for the FORECAST-1 cohort are provided in Tables S7 and S4. WGS for 17 PDTOs with available paired blood samples confirmed tumor origin (Figure S2).

A process for standardized reporting of PDTO-guided treatment recommendations was developed involving assessment of PDTO assay results by a team of study medical oncologists and platform specialists. To facilitate communication of overall PDTO sensitivity patterns to clinicians, and after input from a broader medical oncology panel including all trial site investigators, data were summarized in graphical format with treatments grouped into quintiles from low to high sensitivity based on our reference treatment-naive community cohort (Figure 5B); PDTO assay cutoff-based predictions of sensitivity and resistance will be formally indicated in future versions of the report. Clinical interpretation considered assay predictions and the level of clinical trial evidence for each drug; a higher sensitivity score was given to agents with proven activity in randomized clinical trials versus those with limited prospective data supporting rechallenge strategies versus agents with activity indicated in non-randomized phase 2 studies. To summarize clinical recommendations, drugs were grouped into categories of predicted highest, intermediate, or lowest clinical benefit (Figure 5B). Study team meetings were convened within 1–8 days (mean, 4 days) of each PDTO assay completion, with all reports prepared within 24 h of this meeting, demonstrating process feasibility. Given the observational nature of this study to determine PDTO assay accuracy in the context of current standard treatment, PDTO assay results were not used to direct treatment, with patients receiving palliative therapy as per clinician's discretion.

Of the 19 AGITG FORECAST-1 patients with PDTO assay results, 11 commenced palliative treatment post-biopsy, with 4 patients ultimately receiving multiple post-biopsy treatment lines. A total of 10 treatment responses of 9 patients were evaluable (TAS-102, n = 4; FOLFOX/CAPOX, n = 3; FOLFOX + bevacizumab, n = 1; and FOLFIRI + cetuximab/panitumumab, n = 2). All 10 PDTO

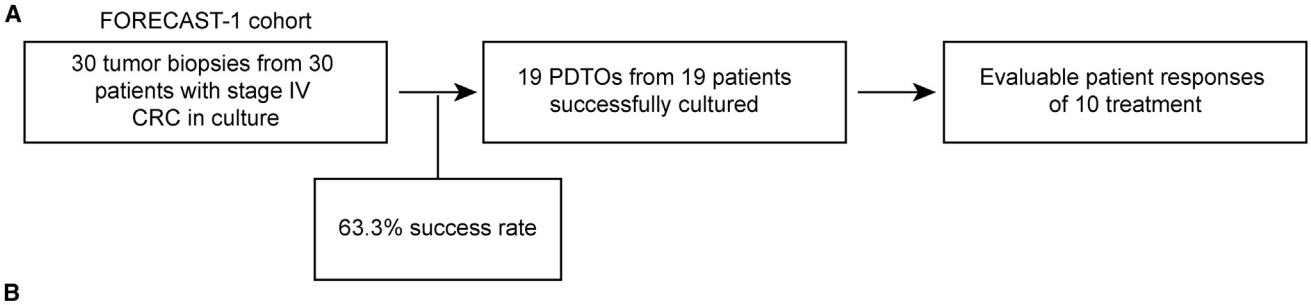

B

	Drug	Relative sensitivity
Ph III RCT demonstrating survival benefit	TAS102	●
	Regorafenib	●
Limited prospective data supporting rechallenge strategies	Oxaliplatin	●
	Irinotecan	●
	5FU/fluoropyrimidine	●
Limited evidence for treatment in refractory setting	Pemetrexed	●
	Gemcitabine	●
	Temozolomide	●
		Less sensitive ← Intermediate sensitivity → More sensitive

Efficacy	Therapeutic agent
Highest possibility of clinical benefit	5FU/fluoropyrimidine
	Oxaliplatin
Intermediate possibility of clinical benefit	TAS102
Lower possibility of clinical benefit	Regorafenib
	Irinotecan
	Pemetrexed
	Gemcitabine
	Temozolomide

C

Patient	Chemotherapy	Targeted therapy
WCB250	FOLFOX	
WCB251	TAS102	
WCB259	TAS102	
WCB259	CAPOX	
WCB262	FOLFIRI	Panitumumab
WCB272	TAS102	
WCB278	FOLFIRI	Cetuximab
WCB281	TAS102	
WCB288	FOLFOX	Bevacizumab
WCB311	FOLFOX	

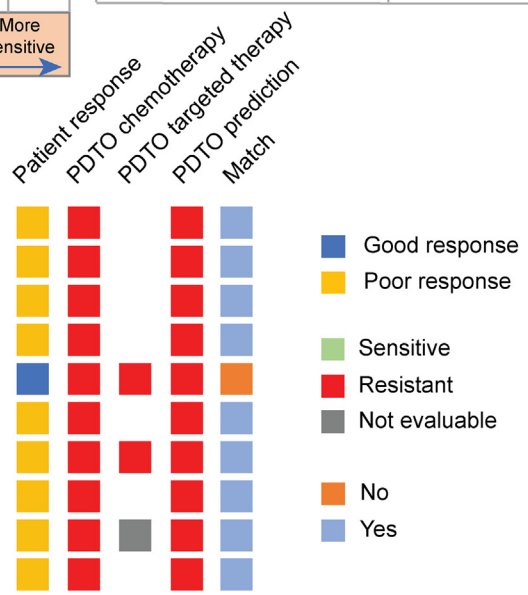

Figure 5. AGITG FORECAST-1 study to determine the feasibility of PDTO-based response prediction in the third-line or later mCRC treatment setting

(A) Flow chart indicating the number of patients recruited, the success rate of establishing and drug testing PDTO cultures, and the number of evaluable patients and clinical responses.

(B) Representative report indicating PDTO assay results for single-agent treatments grouped into quintiles from low to high sensitivity and summary of respective moderated clinical interpretations; future versions of the report will indicate PDTO assay cutoff-based predictions of sensitivity and resistance.

(C) Details of patient treatments, clinical outcomes, PDTO predictions, and matching status of predictions and responses (9 patients, 10 treatments).

See also Figures S1 and S2 and Tables S4, S6, S7, and S8.

assay predictions indicated "resistance" and correctly identified 9 treatments that did not yield clinical benefit, thus achieving a 90% accuracy (Figure 5C). PDTO assay results were obtained prior to commencement of evaluable treatments in 20% (2 of 10) cases. Notably, PDTO testing identified treatments potentially efficacious for 9 of 19 AGITG FORECAST-1 patients (Table S8).

One patient received off-label treatment with gemcitabine after exhausting standard-of-care therapy options; respective PDTO

sensitivity to gemcitabine corresponded to the 61st percentile of responses as observed in our treatment-naive community reference cohort, with the patient developing PD after 126 days on therapy.

PDTO assay predictions by treatment regimen and successive lines of therapy

Combining our AGITG FORECAST-1 cohort and community patients receiving palliative treatment (27 patients, 39 evaluable treatments), PDTO assays achieved a prediction accuracy of 84.6% (95% CI = 69.5%–94.1%; p value [Acc > NIR] < 0.001) with 66.7% sensitivity, 95.8% specificity, 82.1% negative predictive value (NPV), and 90.9% positive predictive value (PPV) (Figure 6A). Incorrectly classified cases were not associated with any particular treatment regimen (5FU/capecitabine ± bevacizumab, 1 of 8, 12.5%; FOLFIRI/XELIRI [capecitabine and irinotecan] ± bevacizumab, 0 of 3, 0%; FOLFIRI/XELIRI + cetuximab/panitumumab, 1 of 4, 25.0%; FOLFOX/CAPOX [capecitabine and oxaliplatin] ± bevacizumab, 1 of 10, 10.0%; FOLFOX/CAPOX + cetuximab/panitumumab, 1 of 2, 50.0%; FOLFOXIRI, 0 of 3, 0%; TAS-102, 1 of 8, 12.5%). Patients receiving treatments associated with "resistant" PDTO predictions exhibited inferior progression-free survival (PFS) as compared to those receiving treatments associated with "sensitive" PDTO predictions with a hazard ratio (HR) of 3.97 (95% CI = 1.36–11.57; p = 0.007, log-rank test) (Figure 6B). This survival trend was maintained when adjusting analysis for treatment with single versus combination chemotherapy (HR = 3.63, 95% CI = 1.23–10.76, p = 0.020). Previous PDTO studies of drug combination treatments indicate that analyzing combination matrices, rather than each drug separately, more accurately discriminates patient clinical responses.[11] Accordingly, for FOLFOX and FOLFIRI treatments, our combined cohort analysis showed higher concordance of drug combination matrices with treatment responses (84.2%, 16 of 19) as compared to single-agent components (63.2%, 12 of 19) (Figure S3).

Finally, we probed for impact of treatments in modulating responses to further therapy in exploratory analysis. PDTOs generated from patients who were refractory to 5FU-based regimens in previous lines of therapy (5FU/FOLFIRI/FOLFOX, n = 33) were less sensitive to 5FU-based regimens as compared to PDTOs from treatment-naive patients (n = 56), but this did not appear to influence sensitivity to unrelated treatment regimens (Figure 6C). With guidelines for mCRC treatment favoring successive use of unrelated therapy options, we did not observe increased misclassification rates with successive patient treatments post-PDTO assay, although sample size was limited (18.5%, 5 of 27 for immediate lines versus 8.3%, 1 of 12 for subsequent lines) (Figure S4). Accordingly, the overall trend to inferior PFS for patients with "resistant" PDTO predictions was maintained when adjusting analysis for immediate versus subsequent treatment lines (HR = 3.96, 95% CI = 1.36–11.56, p = 0.012).

PDTO assay miniaturization to reduce time from biopsy to drug screen result

A limitation of our comprehensive PDTO assay setup highlighted in AGITG FORECAST-1 was the time taken from tissue biopsy to drug screen results. With input cell number being the main limiting factor, we explored reduction of dose titration points by selecting concentration windows for single agents and combinations at which the variance of *in vitro* drug sensitivity profiles was the largest for our treatment-naive reference cohort. We then performed response prediction for our independent AGITG FORECAST-1 cohort and community patients receiving palliative treatments (27 patients, 39 evaluable treatments).

Prediction accuracies are detailed for decreasing titration window sizes from 5 to 2 single points in Table S9. Across all window sizes, PDTO assay performance and association with PFS improved as compared to the original full dose titrations (Figures 7A and 7B), indicating that a 2-point window was adequate for miniaturization of standard-of-care drug testing (requiring ~144,000 cells). Based on PDTO establishment rates and growth trajectories observed for AGITG FORECAST-1 biopsy samples, this would enable assay results to be generated within a 7-week time frame for 68.8% (11 of 16) patients with CRC liver metastasis but only 28.6% (4 of 14) patients with metastases from other sites (Figure 7C).

DISCUSSION

In this study, we have developed a unified framework for predictive PDTO standard-of-care drug testing and clinical reporting of drug sensitivity for patients with mCRC. Previous prospective studies have investigated PDTO assays for limited chemotherapy options with training based on observed clinical responses, including first-line 5FU-oxaliplatin and second-line irinotecan-based treatment (TUMOROID study[13]) or joint prediction for neoadjuvant and adjuvant FOLFOX/FOLFIRI/FOLFOXIRI therapy.[21] In contrast, we developed a predictive PDTO assay approach applicable across standard-of-care chemotherapy and biologic and targeted therapy options derived from a combination of PDTO assay results from an initial cohort of treatment-naive CRC community patients and response rates reported in first-line mCRC clinical trials. Successful application in an independent community-based cohort of patients with mCRC receiving routine palliative treatment achieved an overall PDTO assay accuracy of 83%. Further prospective validation of our PDTO assay framework in the AGITG FORECAST-1 study of third-line or later-line mCRC treatment also achieved 90% accuracy, although the number of evaluable patients was limited, and expanded validation studies will be required to further validate assay accuracy statistics. While AGITG FORECAST-1 was an observational study, alternative, potentially efficacious treatment options were identified for 9 of 19 patients with PDTO assay results.

Consistent with studies propagating PDTOs in Matrigel domes,[14,18,34] PDTOs grown in LVM culture conditions exhibited similar marker expression as the original tumor, including Ki67 proliferative index and staining patterns for p53 and Muc2. Our genome-wide sequencing analysis showed a median SNV overlap of 72.2% (range, 49.4%–87.8%) between PDTO and matched tumor samples. A previous study by van de Wetering et al. assessing exome-wide SNV overlap between PDTOs and original tumors had reported a median concordance of 88% (range, 62%–100%) but with manual curation of mutation data[34]; re-examination of deposited mutation calls using the same *in silico* filtering approach

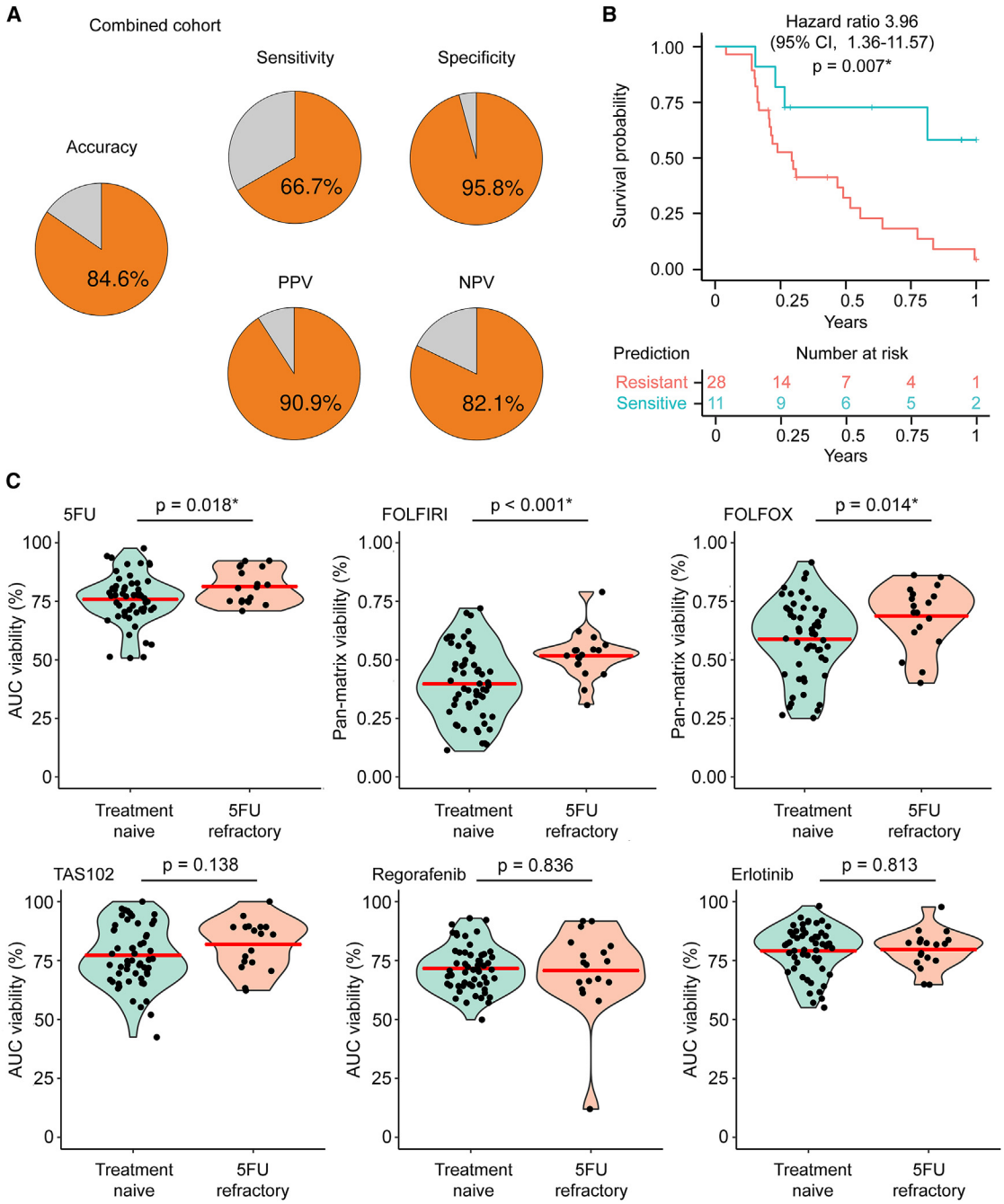

Figure 6. PDTO assay predictions for the combined AGITG FORECAST-1 and community mCRC patient cohorts

(A) Pie charts detailing PDTO assay accuracy, sensitivity, specificity, PPV, and NPV for 27 patients with mCRC with 39 evaluable treatments.

(B) Kaplan-Meier plot of progression-free survival divided into sensitive and resistant groups according to PDTO assay predictions. Statistical significance was attributed to values of $p < 0.050$ as determined by the log-rank test.

(C) Comparison of drug sensitivity between PDTOs from chemo-naive patients (n = 56) and PDTOs from patients refractory to 5FU-based treatment (5FU, FOLFIRI, and FOLFOX; n = 18) for 5FU, FOLFIRI, FOLFOX, TAS-102, regorafenib, and erlotinib. Statistical significance was attributed to values of $p < 0.050$ as determined by Student's t test. *$p < 0.050$.

See also Figures S3 and S4.

as for our analysis yielded a median SNV overlap of 85.7% (range, 0.0%–97.6%) (Figure S5A). Moreover, analysis of deposited exome sequencing data on PDTOs and matched tumors from Yao et al. yielded a median SNV overlap of 76.3% (range, 26.8%–92.8%), similar to our findings (Figure S5B).[14] Consistent with other studies,[12,14,16,34] we observed a high concordance

CellPress
OPEN ACCESS

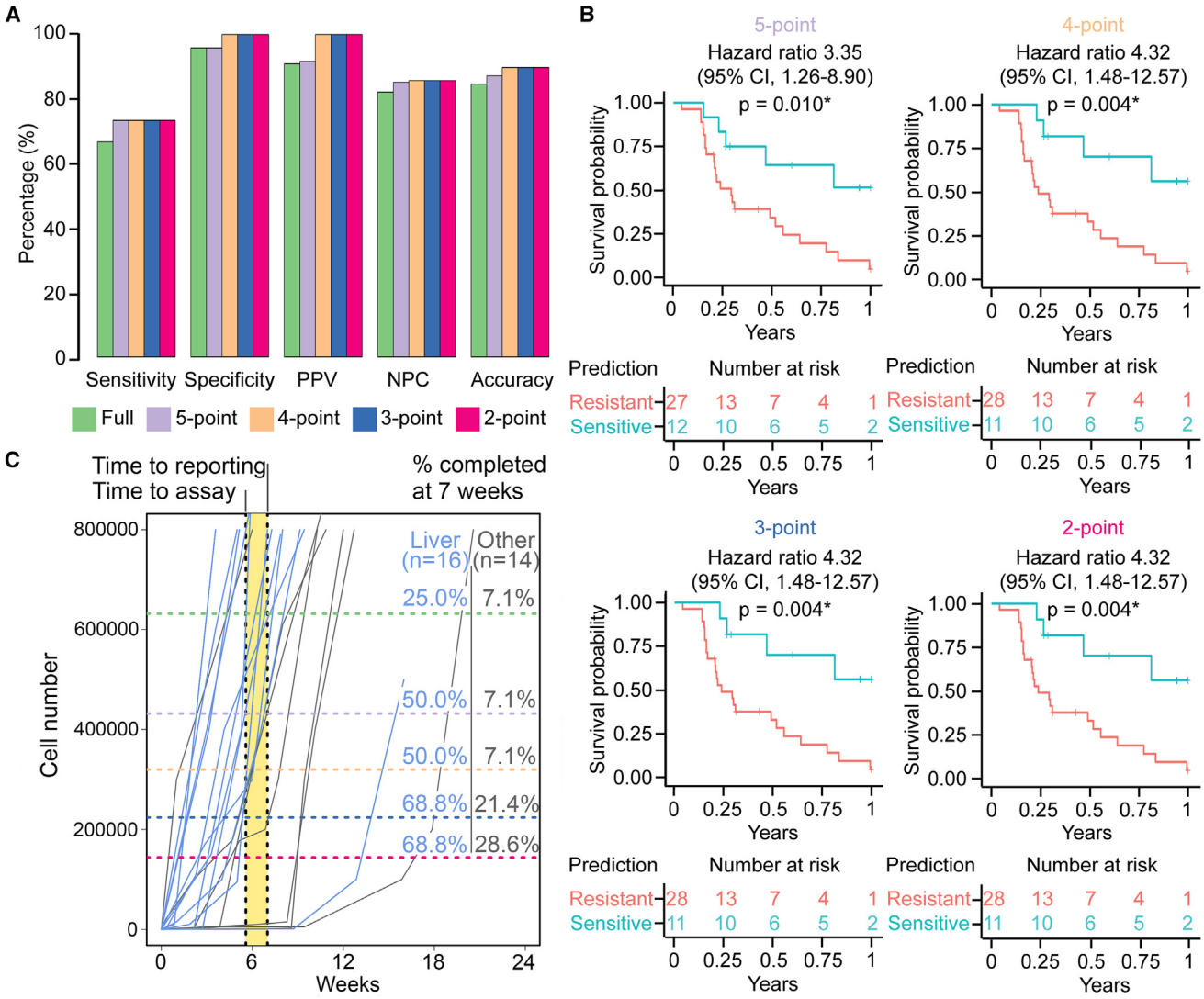

Figure 7. PDTO assay miniaturization to reduce time from biopsy to drug screen result

(A) PDTO assay sensitivity, specificity, PPV, NPV, and accuracy for decreasing drug titration window sizes from 5 to 2 single points for 27 patients with mCRC with 39 evaluable treatments from the combined AGITG FORECAST-1 and community mCRC patient cohorts.

(B) Kaplan-Meier plot of progression-free survival divided into sensitive and resistant groups according to PDTO assay predictions for decreasing window sizes. Statistical significance was attributed to values of $p < 0.050$ as determined by the log rank test. *$p < 0.050$.

(C) Growth curves of successfully assayed PDTOs from AGITG FORECAST-1 biopsy samples. Horizontal dashed lines indicate the number of cells required to test PDTOs for standard-of-care treatments for decreasing assay window sizes. Vertical dashed lines indicate time to PDTO assay commencement with reporting at 7 weeks. CRC liver metastases are shown in blue, and metastases from other sites are in gray. Percentages of biopsy samples estimated to be tested and reported within 7 weeks are shown for liver and other metastatic sites.

See also Table S9.

for the mutational spectrum in major CRC driver genes (97.5%, range, 81.0–100%). In our study, two cases (WCB266 and WCB088) had more discordant SNV profiles between the PDTO and the tumor; both cases were non-hypermutated, with discordance likely related to clonal molecular heterogeneity as previously reported by others.[35,36]

Previous studies sampling CRC biopsies from metastatic sites have reported culture success rates of 54%–63% using culture methods with PDTO embedment into solid support matrices.[13,37,38] In the AGITG FORECAST-1 study, we achieved a similar 63% overall success rate for PDTO LVM cultures[25] and identified CRC liver metastases as the optimal biopsy site for PDTO generation with a 75% success rate (compared to 50% for other sites). Nonetheless, PDTO culture success rate remains a major barrier to eventual clinical translation with biopsy size, tumor cell content, and viability established as critical factors for success[18,38]; further improvements in PDTO success rate may be achieved by increasing biopsy number and/or size

and by further optimization of culture conditions such as replacement of classic niche factors with emerging biomimetic compounds or introduction of new biopsy methods.[35,39–41]

The duration of PDTO expansion prior to *in vitro* treatments depends on tumor cell proliferation rate and the required cell input and number of assay points.[13,37,38] For AGITG FORECAST-1, we required 4–21 weeks to examine 9 single agents in duplicate 9-step dose titrations and 2 drug combinations in duplicate 7 × 7 matrices. However, PDTO assay miniaturization to a 2-point window was found to maintain and potentially improve prediction accuracy and association with PFS. Based on PDTO establishment and growth rates observed in AGITG FORECAST-1, a 7-week turnaround time for PDTO standard-of-care drug testing thus appears feasible for an estimated 69% patients with CRC liver metastases. This time frame is in line with that of a recent phase 2, single-arm study of PDTO-guided use of investigational agents in refractory mCRC (ClinicalTrials.gov: NCT03251612), which achieved treatment assignment within a median of 51 days from enrollment for 38% study participants and reported improved PFS as compared to benchmark clinical trial data.[37] Additional efforts in assay miniaturization, including exploration of emerging organoid-on-a-chip approaches,[42,43] will be required for PDTO drug sensitivity testing to meet timelines required for clinical implementation.

Although the PDTO assay achieved an overall accuracy of 84.6% with a PPV of 90.9% and an NPV of 82.1% for the combined community and FORECAST- 1 cohorts, sensitivity was limited to 66.7%, with a total of five false negative cases where PDTOs showed resistance while the patients did show clinical benefit. In 2 out of 5 cases, PDTO assay results were close to the prediction cutoff (within 5% viability), indicating *bona fide* misclassification based on the current model; further cutoff tuning with an expanded patient training cohort may improve model performance. In 3 out of 5 cases, assay results demonstrated definitive PDTO resistance, with discordance with patient outcome likely related to clonal heterogeneity as similarly reported in previous studies assessing multiple tumor biopsies or metastatic lesions[13,18,34]; addressing this deficiency will require multiple-lesion sampling and assessment.

Among non-standard-of-care agents for mCRC explored in our study, limited PDTO responsiveness was observed for temozolomide and pemetrexed. However, a subset of PDTOs was sensitive to gemcitabine treatment, consistent with previous data from the APOLLO and ClinicalTrials.gov: NCT03251612 studies.[19,37] One patient treated with gemcitabine in AGITG FORECAST-1 after failure of standard-of-care therapy exhibited PDTO sensitivity corresponding to the 61st percentile of responses in our treatment-naive reference cohort, and this patient demonstrated some treatment benefit, developing PD after 126 days on therapy. Similarly, both the APOLLO and ClinicalTrials.gov: NCT03251612 studies reported evidence of patient benefit for PDTO-guided gemcitabine treatment.[19,37]

While current prospective data indicate that PDTO drug screen results for patients with mCRC are predictive for irinotecan-based treatment,[13,21] findings for oxaliplatin-based treatment remain contentious, with the TUMOROID study indicating poor performance.[13] In combined cohort analysis, we found no evidence of differential misclassification rates between FOLFIRI and FOLFOX treatments; misclassification rates were also largely similar for other treatment regimens, although patient numbers were small, precluding definitive analysis. Future work will be required to more robustly evaluate the clinical utility of our PDTO assay framework across the various treatment lines and regimens for mCRC.

Earlier lines of treatment may influence responses for later treatment lines. Our data demonstrate acquisition of tumor resistance for 5FU-based therapy, but this did not appear to impact sensitivity to other unrelated treatment regimens in our small study cohort. Nonetheless, given this limitation, retesting of PDTOs for later treatment lines remains warranted, as any therapy post-PDTO establishment has the potential to impact response to future post-PDTO treatments.

Current clinical and molecular biomarkers for personalization of mCRC therapy are limited to targeted therapies including left-sided primary cancer location and KRAS/NRAS mutation status for anti-EGFR antibody therapy, *BRAF*^{V600E} mutation status for BRAF-targeted therapies, and HER2/ERBB2 amplification status for HER2-targeted therapies.[2–10] Even among patients treated with genomically guided therapies, response rates are limited, and matching of alternative investigational agents by tumor genomic sequencing alone has proven challenging.[44] Advances in PDTO technology hold promise for guiding use of routine cancer treatments, enabling prediction for chemotherapy agents for which no biomarkers are currently available and complementing genomic testing for targeted therapies. Our framework for predictive PDTO drug sensitivity testing and clinical reporting is adaptable across the range of standard-of-care therapy options and treatment lines for patients with mCRC, but biopsy culture success rate and time to assay results require further improvement for clinical implementation. Although we observed high assay accuracy in AGITG FORECAST-1, patient deterioration and low response rates constrain the benefit of PDTO standard-of-care drug testing to predict response in the typically treatment refractory third-line setting. While there remains opportunity for clinical gains in the late-line setting, particularly for investigational agents, our findings suggest that the greatest potential for standard-of-care PDTO testing is first- and second-line treatment selection, where equipoise exists for multiple therapy options. Implementation in early lines of treatment would provide the greatest opportunity for benefit of PDTO-guided therapy while avoiding the use of ineffective, toxic, and costly treatments. Early exploration of potential alternative investigational approaches would further provide a larger time frame to source off-label agents for patients and to enable accelerated targeted conduct of confirmatory PDTO assays upon failure of standard-of-care therapy options. Ultimately, the clinical benefit and cost effectiveness of PDTO drug testing compared to standard physician-guided treatment will need to be demonstrated in a randomized clinical trial.

Limitations of the study

Limitations of this study include that PDTO growth in culture medium lacking Wnt ligands to prevent the outgrowth of normal epithelium resulted in lower success rates for MMR-deficient tumors, which tend to maintain dependence on Wnt-ligand-mediated Wnt/β-catenin signaling due to the acquisition of loss-of-function mutations in *RNF43*.[45] The determination of

PDTO assay cutoff values on treatment-naive patients included stage I–IV tumors and may be improved in future models solely trained on metastatic samples. Prediction of anti-EGFR antibody response was based on erlotinib as a surrogate, which cannot model antibody-dependent cellular cytotoxicity, although we verified concordance with clinical cetuximab sensitivity and resistance associated with *RAS* mutation status. Currently, there are no data on TAS-102 as a single agent for first-line treatment of patients with mCRC, and objective response rate was estimated based on results of the TASCO-1 trial of TAS-102 plus bevacizumab and first-line data for bevacizumab used in combination with other chemotherapy agents.[46,47] The BRAF inhibitor encorafenib and the HER2-targeted therapies tucatinib and trastuzumab were not assessed in the current study as these were not available to our patients at the time of study conduct. Anti-angiogenic and immune therapies could not be assessed in a monoculture PDTO assay, and assessing sensitivity to these agents will require development of appropriate co-culture assays. While our current data suggest assay utility for diverse standard-of-care regimens based on limited patient numbers, expanded studies will be required to formally demonstrate accuracy for each treatment option. Similarly, our analyses of PFS need to be considered exploratory, with types and sequence of treatments as potential confounders that could only be partly addressed in adjusted analyses.

STAR★METHODS

Detailed methods are provided in the online version of this paper and include the following:

- KEY RESOURCES TABLE
- RESOURCE AVAILABILITY
  - Lead contact
  - Materials availability
  - Data and code availability
- EXPERIMENTAL MODEL AND STUDY PARTICIPANT DETAILS
- METHOD DETAILS
  - PDTO generation
  - Histological assessment
  - Whole genome sequencing and variant calling
  - *RAS*, *RAF* mutation and DNA mismatch repair status
  - Semiautomated PDTO drug assay
- QUANTIFICATION AND STATISTICAL ANALYSIS
- ADDITIONAL RESOURCES

SUPPLEMENTAL INFORMATION

Supplemental information can be found online at https://doi.org/10.1016/j.xcrm.2023.101335.

ACKNOWLEDGMENTS

This study was supported by an Innovation Grant from the Australasian Gastro-Intestinal Trials Group (AGITG), the Stafford Fox Medical Research Foundation, Cancer Australia through the 2017 Priority-driven Collaborative Cancer Research Scheme (GNT1145907), a Beijing Genomics Institute Genome Decode Program grant, an Independent Research Institutes Infrastructure Support Scheme grant, and a Victorian State Government Operational Infrastructure support grant. T.T. is supported by the China Scholarship Council (award number: 201706190314). O.M.S. is a National Health and Medical Research Council Senior Research Fellow (GNT1136119). This work was supported by the Guangdong Provincial Key Laboratory of Human Disease Genomics (2020B1212070028) and by the China National GeneBank with computational and sequencing resources. The FORECAST-1 study was endorsed by the AGITG. The authors thank the Victorian Cancer BioBank and Biogrid Australia for provision of patient specimens and clinical data. The Victorian Cancer Biobank through the Cancer Council Victoria as Lead Agency is supported by the Victorian government through the Victorian Cancer Agency, a business unit of the Department of Health.

AUTHOR CONTRIBUTIONS

Conceptualization, T.T., D.M., M.L., G.G., A.W.B., P.G., and O.M.S.; data curation, T.T., D.M., M.L., G.G., H.B., J.T., N.C.T., A.J., R.W., and P.G.; formal analysis, T.T., D.M., M.L., G.G., P.G., and O.M.S.; funding acquisition, M.L., G.G., A.W.B., P.G., and O.M.S.; investigation, T.T., M.L., G.G., Y.H., S.L., C.L., H.L., K.W., M.P., E.L., J.C., and A.S.; methodology, T.T., D.M., M.L., G.G., C.L., H.L., K.W., P.G., and O.M.S.; project administration, H.B.; supervision, A.W.B., P.G., and O.M.S.; visualization, T.T., D.M., and O.M.S.; writing – original draft, T.T., D.M., and O.M.S.; writing – review & editing, T.T., D.M., M.L., G.G., Y.H., S.L., C.L., F.L., H.L., K.W., M.P., E.L., J.C., A.S., H.B., J.T., N.C.T., A.J., R.W., A.W.B., P.G., and O.M.S.

DECLARATION OF INTERESTS

The authors declare no competing interests.

INCLUSION AND DIVERSITY

We support inclusive, diverse, and equitable conduct of research.

Received: May 17, 2023
Revised: September 11, 2023
Accepted: November 18, 2023
Published: December 19, 2023

REFERENCES

1. Sung, H., Ferlay, J., Siegel, R.L., Laversanne, M., Soerjomataram, I., Jemal, A., and Bray, F. (2021). Global Cancer Statistics 2020: GLOBOCAN Estimates of Incidence and Mortality Worldwide for 36 Cancers in 185 Countries. CA. Cancer J. Clin. *71*, 209–249.
2. Van Cutsem, E., Köhne, C.H., Láng, I., Folprecht, G., Nowacki, M.P., Cascinu, S., Shchepotin, I., Maurel, J., Cunningham, D., Tejpar, S., et al. (2011). Cetuximab plus irinotecan, fluorouracil, and leucovorin as first-line treatment for metastatic colorectal cancer: updated analysis of overall survival according to tumor KRAS and BRAF mutation status. J. Clin. Oncol. *29*, 2011–2019.
3. Tejpar, S., Stintzing, S., Ciardiello, F., Tabernero, J., Van Cutsem, E., Beier, F., Esser, R., Lenz, H.J., and Heinemann, V. (2017). Prognostic and Predictive Relevance of Primary Tumor Location in Patients With RAS Wild-Type Metastatic Colorectal Cancer: Retrospective Analyses of the CRYSTAL and FIRE-3 Trials. JAMA Oncol. *3*, 194–201.
4. Douillard, J.Y., Siena, S., Cassidy, J., Tabernero, J., Burkes, R., Barugel, M., Humblet, Y., Bodoky, G., Cunningham, D., Jassem, J., et al. (2014). Final results from PRIME: randomized phase III study of panitumumab with FOLFOX4 for first-line treatment of metastatic colorectal cancer. Ann. Oncol. *25*, 1346–1355.
5. Peeters, M., Oliner, K.S., Price, T.J., Cervantes, A., Sobrero, A.F., Ducreux, M., Hotko, Y., André, T., Chan, E., Lordick, F., et al. (2015). Analysis of KRAS/NRAS Mutations in a Phase III Study of Panitumumab with FOLFIRI Compared with FOLFIRI Alone as Second-line Treatment for Metastatic Colorectal Cancer. Clin. Cancer Res. *21*, 5469–5479.

6. Le, D.T., Uram, J.N., Wang, H., Bartlett, B.R., Kemberling, H., Eyring, A.D., Skora, A.D., Luber, B.S., Azad, N.S., Laheru, D., et al. (2015). PD-1 Blockade in Tumors with Mismatch-Repair Deficiency. N. Engl. J. Med. *372*, 2509–2520.

7. André, T., Shiu, K.K., Kim, T.W., Jensen, B.V., Jensen, L.H., Punt, C., Smith, D., Garcia-Carbonero, R., Benavides, M., Gibbs, P., et al. (2020). Pembrolizumab in Microsatellite-Instability-High Advanced Colorectal Cancer. N. Engl. J. Med. *383*, 2207–2218.

8. Overman, M.J., Lonardi, S., Wong, K.Y.M., Lenz, H.J., Gelsomino, F., Aglietta, M., Morse, M.A., Van Cutsem, E., McDermott, R., Hill, A., et al. (2018). Durable Clinical Benefit With Nivolumab Plus Ipilimumab in DNA Mismatch Repair-Deficient/Microsatellite Instability-High Metastatic Colorectal Cancer. J. Clin. Oncol. *36*, 773–779.

9. Tabernero, J., Grothey, A., Van Cutsem, E., Yaeger, R., Wasan, H., Yoshino, T., Desai, J., Ciardiello, F., Loupakis, F., Hong, Y.S., et al. (2021). Encorafenib Plus Cetuximab as a New Standard of Care for Previously Treated BRAF V600E-Mutant Metastatic Colorectal Cancer: Updated Survival Results and Subgroup Analyses from the BEACON Study. J. Clin. Oncol. *39*, 273–284.

10. Strickler, J.H., Cercek, A., Siena, S., André, T., Ng, K., Van Cutsem, E., Wu, C., Paulson, A.S., Hubbard, J.M., Coveler, A.L., et al. (2023). Tucatinib plus trastuzumab for chemotherapy-refractory, HER2-positive, RAS wild-type unresectable or metastatic colorectal cancer (MOUNTAINEER): a multicentre, open-label, phase 2 study. Lancet. Oncol. *24*, 496–508.

11. Wensink, G.E., Elias, S.G., Mullenders, J., Koopman, M., Boj, S.F., Kranenburg, O.W., and Roodhart, J.M.L. (2021). Patient-derived organoids as a predictive biomarker for treatment response in cancer patients. npj Precis. Oncol. *5*, 30.

12. Ganesh, K., Wu, C., O'Rourke, K.P., Szeglin, B.C., Zheng, Y., Sauvé, C.E.G., Adileh, M., Wasserman, I., Marco, M.R., Kim, A.S., et al. (2019). A rectal cancer organoid platform to study individual responses to chemoradiation. Nat. Med. *25*, 1607–1614.

13. Ooft, S.N., Weeber, F., Dijkstra, K.K., McLean, C.M., Kaing, S., van Werkhoven, E., Schipper, L., Hoes, L., Vis, D.J., van de Haar, J., et al. (2019). Patient-derived organoids can predict response to chemotherapy in metastatic colorectal cancer patients. Sci. Transl. Med. *11*, eaay2574.

14. Yao, Y., Xu, X., Yang, L., Zhu, J., Wan, J., Shen, L., Xia, F., Fu, G., Deng, Y., Pan, M., et al. (2020). Patient-Derived Organoids Predict Chemoradiation Responses of Locally Advanced Rectal Cancer. Cell Stem Cell *26*, 17–26.e6.

15. Bruun, J., Kryeziu, K., Eide, P.W., Moosavi, S.H., Eilertsen, I.A., Langerud, J., Rosok, B., Totland, M.Z., Brunsell, T.H., Pellinen, T., et al. (2020). Patient-Derived Organoids from Multiple Colorectal Cancer Liver Metastases Reveal Moderate Intra-patient Pharmacotranscriptomic Heterogeneity. Clin. Cancer Res. *26*, 4107–4119.

16. Mo, S., Tang, P., Luo, W., Zhang, L., Li, Y., Hu, X., Ma, X., Chen, Y., Bao, Y., He, X., et al. (2022). Patient-Derived Organoids from Colorectal Cancer with Paired Liver Metastasis Reveal Tumor Heterogeneity and Predict Response to Chemotherapy. Adv. Sci. *9*, e2204097.

17. Kim, J., Koo, B.K., and Knoblich, J.A. (2020). Human organoids: model systems for human biology and medicine. Nat. Rev. Mol. Cell Biol. *21*, 571–584.

18. Vlachogiannis, G., Hedayat, S., Vatsiou, A., Jamin, Y., Fernández-Mateos, J., Khan, K., Lampis, A., Eason, K., Huntingford, I., Burke, R., et al. (2018). Patient-derived organoids model treatment response of metastatic gastrointestinal cancers. Science *359*, 920–926.

19. Narasimhan, V., Wright, J.A., Churchill, M., Wang, T., Rosati, R., Lannagan, T.R.M., Vrbanac, L., Richardson, A.B., Kobayashi, H., Price, T., et al. (2020). Medium-throughput Drug Screening of Patient-derived Organoids from Colorectal Peritoneal Metastases to Direct Personalized Therapy. Clin. Cancer Res. *26*, 3662–3670.

20. Chalabi, M., Fanchi, L.F., Dijkstra, K.K., Van den Berg, J.G., Aalbers, A.G., Sikorska, K., Lopez-Yurda, M., Grootscholten, C., Beets, G.L., Snaebjornsson, P., et al. (2020). Neoadjuvant immunotherapy leads to pathological responses in MMR-proficient and MMR-deficient early-stage colon cancers. Nat. Med. *26*, 566–576.

21. Wang, T., Pan, W., Zheng, H., Zheng, H., Wang, Z., Li, J.J., Deng, C., and Yan, J. (2021). Accuracy of Using a Patient-Derived Tumor Organoid Culture Model to Predict the Response to Chemotherapy Regimens In Stage IV Colorectal Cancer: A Blinded Study. Dis. Colon Rectum *64*, 833–850.

22. Lv, T., Shen, L., Xu, X., Yao, Y., Mu, P., Zhang, H., Wan, J., Wang, Y., Guan, R., Li, X., Li, X., et al. (2023). Patient-derived tumor organoids predict responses to irinotecan-based neoadjuvant chemoradiotherapy in patients with locally advanced rectal cancer. Int. J. Cancer *152*, 524–535.

23. Kosmider, S., Jones, I., Hibbert, M., Hunter, A., McLaughlin, S., Johns, J., Chapman, M., and Gibbs, P. (2008). Towards establishing a national colorectal cancer database: lessons learnt from Bio21 molecular medicine informatics model. ANZ J. Surg. *78*, 803–809.

24. Field, K., Wong, H.L., Shapiro, J., Kosmider, S., Tie, J., Bae, S., Yip, D., McKendrick, J., Nott, L., Desai, J., et al. (2013). Developing a national database for metastatic colorectal cancer management: perspectives and challenges. Intern. Med. J. *43*, 1224–1231.

25. Hirokawa, Y., Clarke, J., Palmieri, M., Tan, T., Mouradov, D., Li, S., Lin, C., Li, F., Luo, H., Wu, K., et al. (2021). Low-viscosity matrix suspension culture enables scalable analysis of patient-derived organoids and tumoroids from the large intestine. Commun. Biol. *4*, 1067.

26. Merl, M., Hoimes, C., Pham, T., and Saif, M.W. (2009). Is there a palliative benefit of gemcitabine plus fluoropyrimidines in patients with refractory colorectal cancer? A review of the literature previously presented: poster at the 2008 Gastrointestinal Cancer Symposium (Abstract No. 512). Expet Opin. Invest. Drugs *18*, 1257–1264.

27. Jiménez-Fonseca, P., Solis, M.P., Garrido, M., Faez, L., Rodriguez, D., Ruiz, A.L., Sanchez Lorenzo, M.L., Uriol, E., Menendez, M.D., and Viéitez, J.M. (2015). Gemcitabine plus capecitabine (Gem-Cape) biweekly in chemorefractory metastatic colorectal cancer. Clin. Transl. Oncol. *17*, 384–392.

28. Cripps, C., Burnell, M., Jolivet, J., Batist, G., Lofters, W., Dancey, J., Iglesias, J., Fisher, B., and Eisenhauer, E.A. (1999). Phase II study of first-line LY231514 (multi-targeted antifolate) in patients with locally advanced or metastatic colorectal cancer: an NCIC Clinical Trials Group study. Ann. Oncol. *10*, 1175–1179.

29. John, W., Picus, J., Blanke, C.D., Clark, J.W., Schulman, L.N., Rowinsky, E.K., Thornton, D.E., and Loehrer, P.J. (2000). Activity of multitargeted antifolate (pemetrexed disodium, LY231514) in patients with advanced colorectal carcinoma: results from a phase II study. Cancer *88*, 1807–1813.

30. Louvet, C., and de Gramont, A. (2004). Pemetrexed in advanced colorectal cancer. Oncology *18*, 56–62.

31. Pietrantonio, F., Perrone, F., de Braud, F., Castano, A., Maggi, C., Bossi, I., Gevorgyan, A., Biondani, P., Pacifici, M., Busico, A., et al. (2014). Activity of temozolomide in patients with advanced chemorefractory colorectal cancer and MGMT promoter methylation. Ann. Oncol. *25*, 404–408.

32. Casale, F., Canaparo, R., Serpe, L., Muntoni, E., Pepa, C.D., Costa, M., Mairone, L., Zara, G.P., Fornari, G., and Eandi, M. (2004). Plasma concentrations of 5-fluorouracil and its metabolites in colon cancer patients. Pharmacol. Res. *50*, 173–179.

33. Liston, D.R., and Davis, M. (2017). Clinically Relevant Concentrations of Anticancer Drugs: A Guide for Nonclinical Studies. Clin. Cancer Res. *23*, 3489–3498.

34. van de Wetering, M., Francies, H.E., Francis, J.M., Bounova, G., Iorio, F., Pronk, A., van Houdt, W., van Gorp, J., Taylor-Weiner, A., Kester, L., et al. (2015). Prospective derivation of a living organoid biobank of colorectal cancer patients. Cell *161*, 933–945.

35. Fujii, M., Shimokawa, M., Date, S., Takano, A., Matano, M., Nanki, K., Ohta, Y., Toshimitsu, K., Nakazato, Y., Kawasaki, K., et al. (2016). A Colorectal Tumor Organoid Library Demonstrates Progressive Loss of Niche Factor Requirements during Tumorigenesis. Cell Stem Cell *18*, 827–838.

36. Demmers, L.C., Kretzschmar, K., Van Hoeck, A., Bar-Epraïm, Y.E., van den Toorn, H.W.P., Koomen, M., van Son, G., van Gorp, J., Pronk, A., Smakman, N., et al. (2020). Single-cell derived tumor organoids display diversity in HLA class I peptide presentation. Nat. Commun. *11*, 5338.

37. Jensen, L.H., Rogatto, S.R., Lindebjerg, J., Havelund, B., Abildgaard, C., do Canto, L.M., Vagn-Hansen, C., Dam, C., Rafaelsen, S., and Hansen, T.F. (2023). Precision medicine applied to metastatic colorectal cancer using tumor-derived organoids and in-vitro sensitivity testing: a phase 2, single-center, open-label, and non-comparative study. J. Exp. Clin. Cancer Res. *42*, 115.

38. Ooft, S.N., Weeber, F., Schipper, L., Dijkstra, K.K., McLean, C.M., Kaing, S., van de Haar, J., Prevoo, W., van Werkhoven, E., Snaebjornsson, P., et al. (2021). Prospective experimental treatment of colorectal cancer patients based on organoid drug responses. ESMO Open *6*, 100103.

39. Fujii, M., Matano, M., Toshimitsu, K., Takano, A., Mikami, Y., Nishikori, S., Sugimoto, S., and Sato, T. (2018). Human Intestinal Organoids Maintain Self-Renewal Capacity and Cellular Diversity in Niche-Inspired Culture Condition. Cell Stem Cell *23*, 787–793.e6.

40. Janda, C.Y., Dang, L.T., You, C., Chang, J., de Lau, W., Zhong, Z.A., Yan, K.S., Marecic, O., Siepe, D., Li, X., et al. (2017). Surrogate Wnt agonists that phenocopy canonical Wnt and beta-catenin signalling. Nature *545*, 234–237.

41. Levy, E.B., Fiel, M.I., Hamilton, S.R., Kleiner, D.E., McCall, S.J., Schirmacher, P., Travis, W., Kuo, M.D., Suh, R.D., Tam, A.L., et al. (2020). State of the Art: Toward Improving Outcomes of Lung and Liver Tumor Biopsies in Clinical Trials-A Multidisciplinary Approach. J. Clin. Oncol. *38*, 1633–1640.

42. Jenkins, R.W., Aref, A.R., Lizotte, P.H., Ivanova, E., Stinson, S., Zhou, C.W., Bowden, M., Deng, J., Liu, H., Miao, D., et al. (2018). Ex Vivo Profiling of PD-1 Blockade Using Organotypic Tumor Spheroids. Cancer Discov. *8*, 196–215.

43. Strelez, C., Chilakala, S., Ghaffarian, K., Lau, R., Spiller, E., Ung, N., Hixon, D., Yoon, A.Y., Sun, R.X., Lenz, H.J., et al. (2021). Human colorectal cancer-on-chip model to study the microenvironmental influence on early metastatic spread. iScience *24*, 102509.

44. Zehir, A., Benayed, R., Shah, R.H., Syed, A., Middha, S., Kim, H.R., Srinivasan, P., Gao, J., Chakravarty, D., Devlin, S.M., et al. (2017). Mutational landscape of metastatic cancer revealed from prospective clinical sequencing of 10,000 patients. Nat. Med. *23*, 703–713.

45. Giannakis, M., Hodis, E., Jasmine Mu, X., Yamauchi, M., Rosenbluh, J., Cibulskis, K., Saksena, G., Lawrence, M.S., Qian, Z.R., Nishihara, R., et al. (2014). RNF43 is frequently mutated in colorectal and endometrial cancers. Nat. Genet. *46*, 1264–1266.

46. Van Cutsem, E., Danielewicz, I., Saunders, M.P., Pfeiffer, P., Argilés, G., Borg, C., Glynne-Jones, R., Punt, C.J.A., Van de Wouw, A.J., Fedyanin, M., et al. (2020). Trifluridine/tipiracil plus bevacizumab in patients with untreated metastatic colorectal cancer ineligible for intensive therapy: the randomized TASCO1 study. Ann. Oncol. *31*, 1160–1168.

47. Botrel, T.E.A., Clark, L.G.d.O., Paladini, L., and Clark, O.A.C. (2016). Efficacy and safety of bevacizumab plus chemotherapy compared to chemotherapy alone in previously untreated advanced or metastatic colorectal cancer: a systematic review and meta-analysis. BMC Cancer *16*, 677.

48. Chen, Y., Chen, Y., Shi, C., Huang, Z., Zhang, Y., Li, S., Li, Y., Ye, J., Yu, C., Li, Z., et al. (2018). SOAPnuke: a MapReduce acceleration-supported software for integrated quality control and preprocessing of high-throughput sequencing data. GigaScience *7*, 1–6.

49. Freed, D., Aldana, R., Weber, J.A., and Edwards, J.S. (2017). The Sentieon Genomics Tools - A fast and accurate solution to variant calling from next-generation sequence data. Preprint at bioRxiv.

50. Li, H. (2013). Aligning sequence reads, clone sequences and assembly contigs with BWA-MEM. Preprint at arXiv.

51. Li, H., Handsaker, B., Wysoker, A., Fennell, T., Ruan, J., Homer, N., Marth, G., Abecasis, G., Durbin, R., and Genome Project Data Processing, S. (2009). The Sequence Alignment/Map format and SAMtools. Bioinformatics *25*, 2078–2079.

52. Van der Auwera, G.A., Carneiro, M.O., Hartl, C., Poplin, R., Del Angel, G., Levy-Moonshine, A., Jordan, T., Shakir, K., Roazen, D., Thibault, J., et al. (2013). From FastQ data to high confidence variant calls: the Genome Analysis Toolkit best practices pipeline. Curr Protoc Bioinformatics *43*, 11.10.1–11.10.33.

53. Priestley, P., Baber, J., Lolkema, M.P., Steeghs, N., de Bruijn, E., Shale, C., Duyvesteyn, K., Haidari, S., van Hoeck, A., Onstenk, W., et al. (2019). Pan-cancer whole-genome analyses of metastatic solid tumours. Nature *575*, 210–216.

54. Cameron, D.L., Baber, J., Shale, C., Valle-Inclan, J.E., Besselink, N., van Hoeck, A., Janssen, R., Cuppen, E., Priestley, P., and Papenfuss, A.T. (2021). GRIDSS2: comprehensive characterisation of somatic structural variation using single breakend variants and structural variant phasing. Genome Biol. *22*, 202.

55. Shale, C., Cameron, D.L., Baber, J., Wong, M., Cowley, M.J., Papenfuss, A.T., Cuppen, E., and Priestley, P. (2022). Unscrambling cancer genomes via integrated analysis of structural variation and copy number. Cell Genomics *2*.

56. Schindelin, J., Arganda-Carreras, I., Frise, E., Kaynig, V., Longair, M., Pietzsch, T., Preibisch, S., Rueden, C., Saalfeld, S., Schmid, B., et al. (2012). Fiji: an open-source platform for biological-image analysis. Nat. Methods *9*, 676–682.

57. R Development Core Team (2022). R: A Language and Environment for Statistical Computing (R Foundation for Statistical Computing). https://www.R-project.org/.

58. Chen, F.Z., You, L.J., Yang, F., Wang, L.N., Guo, X.Q., Gao, F., Hua, C., Tan, C., Fang, L., Shan, R.Q., et al. (2020). CNGBdb: China National GeneBank DataBase. Yi Chuan *42*, 799–809.

59. Guo, X., Chen, F., Gao, F., Li, L., Liu, K., You, L., Hua, C., Yang, F., Liu, W., Peng, C., et al. (2020). CNSA: a data repository for archiving omics data. Database *2020*.

60. Tan, T., Hirokawa, Y., Clarke, J., Sakthianandeswaren, A., and Sieber, O.M. (2022). Low-viscosity Matrix Suspension Culture for Human Colorectal Epithelial Organoids and Tumoroids. Bio. Protoc. *12*, e4394.

61. Ponnapalli, S.P., Bradley, M.W., Devine, K., Bowen, J., Coppens, S.E., Leraas, K.M., Milash, B.A., Li, F., Luo, H., Qiu, S., et al. (2020). Retrospective clinical trial experimentally validates glioblastoma genome-wide pattern of DNA copy-number alterations predictor of survival. APL Bioeng. *4*, 026106.

62. Boland, C.R., Thibodeau, S.N., Hamilton, S.R., Sidransky, D., Eshleman, J.R., Burt, R.W., Meltzer, S.J., Rodriguez-Bigas, M.A., Fodde, R., Ranzani, G.N., and Srivastava, S. (1998). A National Cancer Institute Workshop on Microsatellite Instability for cancer detection and familial predisposition: development of international criteria for the determination of microsatellite instability in colorectal cancer. Cancer Res. *58*, 5248–5257.

63. Lindor, N.M., Burgart, L.J., Leontovich, O., Goldberg, R.M., Cunningham, J.M., Sargent, D.J., Walsh-Vockley, C., Petersen, G.M., Walsh, M.D., Leggett, B.A., et al. (2002). Immunohistochemistry versus microsatellite instability testing in phenotyping colorectal tumors. J. Clin. Oncol. *20*, 1043–1048.

64. Harris, P.A., Taylor, R., Thielke, R., Payne, J., Gonzalez, N., and Conde, J.G. (2009). Research electronic data capture (REDCap)–a metadata-driven methodology and workflow process for providing translational research informatics support. J. Biomed. Inf. *42*, 377–381.

STAR★METHODS

KEY RESOURCES TABLE

REAGENT or RESOURCE	SOURCE	IDENTIFIER
Antibodies		
Mouse anti-Ki67 antibody	DAKO	Cat#M7240, RRID: AB_2142367
Mouse anti-MUC2 antibody	Santa Cruz Biotechnology	Cat#sc-7314, RRID: AB_627970
Mouse anti-p53 antibody	Santa Cruz Biotechnology	Cat#sc-126, RRID: AB_628082
Biological samples		
Human colorectal cancer tissues	This paper	N/A
Human normal colon tissues	This paper	N/A
Buffy coat from patient blood samples	This paper	N/A
Chemicals, peptides, and recombinant proteins		
GlutaMax supplement	Gibco	Cat#35050061
HEPES	Sigma-Aldrich	Cat#H3375-1KG
B-27 supplement	Life Technologies	Cat#17504001
N2 supplement	Life Technologies	Cat#17502001
Nicotinamide	Sigma-Aldrich	Cat#72340-1KG
N-acetyl-L-cysteine	Sigma-Aldrich	Cat#A7250-1KG
Recombinant human basic FGF	Life Technologies	Cat#PHG0263
Recombinant human EGF	Life Technologies	Cat#PHG0313
A83-01	Tocris Bioscience	Cat#2939
Primocin	Invivogen	Cat#ant-pm-2
Y27632	Stemcell Technologies	Cat#72308
Matrigel	Corning	Cat#356234
Penicillin-streptomycin	Life Technologies	Cat#15140122
Normocin	Invivogen	Cat#ant-nr-2
Dispase II	Life Technologies	Cat#17105-041
Collagenase IV	Life Technologies	Cat#17104019
TrypLE Express enzyme	Thermo Fisher Scientific	Cat#12604021
Tissue-Tek O.C.T Compound	Emgrid	Cat#4583
HistoGel	Themo Fisher Scientific	Cat#22-110-678
Critical commercial assays		
ISOLATE II Genomic DNA Kit	Bioline	Cat#BIO-52067
DIPSEQ platform (BGI)	BGI	N/A
MGIEasy Universal DNA Library Prep Set	MGI	Cat#1000006986
LookOut Mycoplasma PCR Detection Kit	Sigma-Aldrich	MP0035-1KT
Dako Omnis platform	Agilent	N/A
Deposited data		
Whole genome sequencing data	This paper; The CNGB Sequence Archive (CNSA) of China National GeneBank DataBase (CNGBdb)	Accession numbers of whole-genome sequencing data in CNGBdb: CNP0001424 and CNP0003751 (https://db.cngb.org/cnsa/)
hg38	GCA_000001405.15_GRCh38_no_alt_analysis_set.fna downloaded from HMFTools-Resources	https://nextcloud.hartwigmedicalfoundation.nl/s/LTiKTd8XxBqwaiC?path = %2FHMFTools-Resources
Experimental models: Organisms/strains		
Patient-derived colorectal cancer organoids	This paper	N/A

(*Continued on next page*)

CellPress
OPEN ACCESS

Continued

REAGENT or RESOURCE	SOURCE	IDENTIFIER
Software and algorithms		
SOAPnuke (v2.1.7)	Chen et al.[48]	https://github.com/BGI-flexlab/SOAPnuke/releases/tag/SOAPnuke2.1.7
Sentieon Genomics software (version: sentieon-genomics-202112)	Freed et al.[49]	https://support.sentieon.com/versions/202112/manual/DNAseq_usage/dnaseq/
BWA MEM	Li et al.[50]	https://arxiv.org/abs/1303.3997
Samtools	Li et al.[51]	https://samtools.sourceforge.net/
Picard	"Picard Toolkit." 2019. Broad Institute, GitHub Repository.	http://broadinstitute.github.io/picard/; RRID:SCR_006525
GATK	Van der Auwera et al.[52]	https://currentprotocols.onlinelibrary.wiley.com/doi/10.1002/0471250953.bi1110s43
Hartwig tools	Priestley et al.[53]	https://github.com/hartwigmedical/hmftools
HMFTools-Resources	Hartwig Medical Foundation	https://nextcloud.hartwigmedicalfoundation.nl/s/LTiKTd8XxBqwaiC?path = %2FHMFTools-Resources
SAGE (v3.0.1)	Priestley et al.[53]	https://github.com/hartwigmedical/hmftools/tree/master/sage
PAVE (v1.2.1)	Hartwig Medical Foundation	https://github.com/hartwigmedical/hmftools/releases/tag/pave-v1.2
GRIDSS (v2.13.2-1)	Cameron et al.[54]	https://github.com/PapenfussLab/gridss
GRIPSS (v2.1)	Hartwig Medical Foundation	https://github.com/hartwigmedical/hmftools/releases/tag/gripss-v2.1
PURPLE (v3.4)	Priestley et al.[53]	https://github.com/hartwigmedical/hmftools/releases/tag/purple-v3.4
AMBER (v3.9)	Priestley et al.[53]	https://github.com/hartwigmedical/hmftools/releases/tag/amber-v3.9
COBALT (v1.13)	Priestley et al.[53]	https://github.com/hartwigmedical/hmftools/releases/tag/cobalt-v1.13
LINX (v1.19)	Shale et al.[55]	https://github.com/hartwigmedical/hmftools/releases/tag/linx-v1.19
ImageJ software (NIH Image)	Schindelin et al.[56]	https://ImageJ.nih.gov/ij/
R (version 4.2.0)	R Development Core Team[57]	https://www.R-project.org/
NIS-Elements AR software (version 5.21.03, 64-bit)	Nikon	N/A
Other		
MANTIS Microfluidic Liquid Dispenser	Formulatrix	Cat#0695
JANUS G3 Liquid Handler Workstation	PerkinElmer	G3
384 PinTool addition accessory	PerkinElmer	N/A
Nikon Eclipse Ti2 Inverted Microscope System	Nikon	Eclipse Ti2

RESOURCE AVAILABILITY

Lead contact

Further information and requests for resources and reagents should be directed to and will be fulfilled by the lead contact, Oliver Sieber (sieber.o@wehi.edu.au).

Materials availability

This study did not generate new unique reagents.

Data and code availability

- Whole-genome sequencing data have been deposited in the CNGB Sequence Archive (CNSA) of CNGBdb (https://db.cngb.org/cnsa/)[58,59] and are publicly available. Accession numbers are listed in the key resources table. Drug sensitivity test results have been provided as Table S4.

- This paper does not report the original code.
- Any additional information required to reanalyze the data reported in this paper is available from the lead contact upon request.

EXPERIMENTAL MODEL AND STUDY PARTICIPANT DETAILS

The community cohort included 167 patients with stage I to IV CRC treated at the Royal Melbourne Hospital, Western Health, Eastern Health and the Northern Hospital in Melbourne, Australia, between May 1, 2017 and August 31, 2022; primary or metastatic tumor tissues and adjacent normal tissues were harvested at surgery or routine biopsy. All patients received standard treatment with clinical and outcome data routinely collected by the Australian Comprehensive Cancer Outcomes and Research Database for Colorectal Cancer (ACCORD-CRC) and Treatment of Recurrent and Advanced Colorectal Cancer (TRACC) Registry.[23,24] All patients provided written informed consent, and the study was approved by medical ethics committees at all sites (HREC 2016.249, WEHI).

AGITG FORECAST-1 was a prospective, observational clinical study comprising 30 patients with mCRC who had failed $\geq$ two lines of therapy (Clinical Trial Registration Number: ACTRN12620001353987). AGITG FORECAST-1 included the patient recruiting sites above as well as LaTrobe Regional Health service. Inclusion criteria included patient age >18 years, ability to provide informed consent, ability to safely undergo biopsy to provide fresh tumor samples, ECOG performance status of 0–2, adequate major organ function, fitness for further systemic treatment, failure of or intolerance to standard therapies (prior exposure to trifluridine/tipiracil was not required), discontinuation of prior systemic treatment at least 2 weeks prior to study biopsy, a life expectancy of >3 months, and accessibility for follow up and de-identified coded data collection. All patients were treated with palliative therapy at clinician discretion.

Patient characteristics for the community and FOREACST-1 cohorts including sex and age are provided in Tables S1 and S6.

PDTOs were authenticated using whole genome sequencing data, with matched normal colon tissues or matched buffy coat from patient blood samples as reference samples. All PDTO cultures were confirmed to be mycoplasma negative using the LookOut Mycoplasma PCR Detection Kit (Sigma-Aldrich, MP0035-1KT).

METHOD DETAILS

PDTO generation

PDTOs were generated in low-viscosity matrix (LVM) suspension culture medium as described previously.[25,60] Tumor samples obtained at resection or biopsy were washed 3–5 times with PBS, minced with scissors into pieces that can pass through 1-mL tips, digested at 37°C for 30–60 min with 0.1 mg/mL Dispase II (Life Technologies, 17105-041) and 200 U/ml Collagenase IV (Life Technologies, 17104019) in DMEM/F12 (Life Technologies, 11320082), and then washed with PBS for another 5–10 times at 200 g for 3 min before being plated into 6-well plates (Interpath, 657185) in PDTO LVM culture medium consisting of advanced DMEM/F12 (Thermo Fisher Scientific, 12634028), 1x GlutaMax supplement (Gibco, 35050061), 10 mM HEPES (Sigma-Aldrich, H3375-1KG), 1x B-27 supplement (Life Technologies, 17504001), 1x N2 supplement (Life Technologies, catalog number: 17502001), 10 mM nicotinamide (Sigma-Aldrich, 72340-1KG), 1 mM N-acetyl-L-cysteine (Sigma-Aldrich, A7250-1KG), 20 ng/mL recombinant human basic FGF (Life Technologies, PHG0263), 50 ng/mL recombinant human EGF (Life Technologies, PHG0313) and 500 nM A83-01 (Tocris Bioscience, 2939), with the addition of 100 μg/mL primocin, 10 μM Y27632 (Stemcell Technologies, 72308) and 5% Matrigel (Corning, 356234). PDTOs were cultured at 37°C in 5% CO_2. Culture medium was changed every 2–3 days and PDTO cultures were agitated by pipetting to prevent adhesion of organoids to the wells.

For passaging, PDTOs were collected, washed with PBS at 200 g for 3 min, digested with TrypLE Express enzyme (Thermo Fisher Scientific, 12604021) at 37°C for 10–15 min with mechanical agitation every 5 min, washed with advanced DMEM/F12 at 200 g for 3 min, and plated in PDTO culture medium containing 100 U/ml penicillin-streptomycin (Life technologies, 15140122), 100 μg/mL normocin (Invitrogen, ant-nr-2).

For cryopreservation in liquid nitrogen, PDTOs cultured for 3–7 days were harvested, washed with PBS at 200 g for 3 min, resuspended in CryoStor CS10 cell freezing medium (STEMCELL Technologies, 7930) and frozen at the cooling rate of 1°C per minute in a Corning CoolCell LX Cell Freezing Container (Biocision, BCS-405) at −80°C. For long-term storage, frozen cells were transferred to liquid nitrogen.

Histological assessment

To prepare samples for histology, pieces of fresh CRC tissue samples were embedded in Tissue-Tek O.C.T Compound (Emgrid, 4583) and rapidly frozen by isopropyl bath on dry ice. Formalin-fixed paraffin-embedded CRC tissue samples were retrieved from pathology archives. PDTOs grown for 2–4 weeks since last passaging were collected at 200 g for 3 min, washed once with PBS at 200 g for 3 min, resuspended in pre-warmed HistoGel (thawed at 95°C and keep at 55°C before usage) (Themo Fisher Scientific, 22-110-678), fixed in 10% formalin at 4°C overnight and then preserved in PBS at 4°C until sent for paraffin embedment by WEHI histology facility. All histology samples were sectioned and stained with hematoxylin and eosin (H&E).

Immunohistochemistry (IHC) was performed on a Dako Omnis platform by WEHI histology facility. For Ki67 staining, anti-Ki67 antibody (1:100, clone MIB-1, DAKO, M7240) was used; for p53 staining, anti-p53 antibody (1:100, clone DO-1, Santa Cruz Biotechnology, sc-126) was used after antigen retrieval for section slides in low PH solution (DAKO, K800521-2) at 97°C for 30 min; for Mucin

2 staining, anti-MUC2 antibody (1:100, clone CCP58, Santa Cruz Biotechnology, sc-7314) was used after antigen retrieval for section slides in low PH solution at 97°C for 30 min. Slides were scanned on a 3D Histech Panoramic Scan II histology scanner (3DHISTECH Ltd.) and image data were stored and examined using CaseViewer Software (3DHISTECH Ltd.).

Whole genome sequencing and variant calling

DNA was extracted from fresh-frozen tissue or blood samples with the ISOLATE II Genomic DNA Kit (Bioline, BIO-52067); tumor samples were confirmed to comprise greater than 60% neoplastic cell content by inspection of H&E-stained sections. A total of 97 samples, 21 trios (adjacent normal tissue, tumor tissue and tumor organoid) from the community cohort and 17 pairs (blood and tumor organoid) from the AGITG FORECAST-1 study, were sequenced on a DIPSEQ platform (BGI). Sequencing libraries were constructed using the MGIEasy Universal DNA Library Prep Set (MGI, 1000006986) and 2 x 100-bp paired-end sequencing was performed to yield data of estimated $\geq$30 x coverage.[61]

Data pre-processing, including removal of low-quality reads and adaptor sequences, was carried out using SOAPnuke (v2.1.7).[48] High quality reads were mapped and processed for downstream analysis using Sentieon Genomics software (version: sentieon-genomics-202112)[49] which includes the following optimized steps: 1) aligned hg38 (GCA_000001405.15_GRCh38_no_alt_analysis_set.fna downloaded from HMFTools-Resources) with BWA MEM[50]; 2) sorted alignment reads by Samtools[51]; 3) marked duplicate reads by Picard (http://broadinstitute.github.io/picard/); 4) indel realignment and base quality score recalibration for alignment reads by GATK[52]; and 5) alignment QC by Picard.

Variants of paired samples (adjacent normal tissue vs. tumor tissue and adjacent normal tissue vs. tumor organoid) were called by series of Hartwig tools (https://github.com/hartwigmedical/hmftools).[53] Resource files of GRCh38 for Hartwig tools were downloaded from HMFTools-Resources (https://nextcloud.hartwigmedicalfoundation.nl/s/LTiKTd8XxBqwaiC?path=%2FHMFTools-Resources) on March 10, 2022. SAGE (v3.0.1)[53] and PAVE (v1.2.1) were used to call and annotate somatic and germline short variants (SNVs, MNVs and INDELs). GRIDSS[54] (https://github.com/PapenfussLab/gridss, v2.13.2-1) and GRIPSS (v2.1) were used to call and filter simple and complex somatic SVs. PURPLE (v3.4)[53] combines B-allele frequency (BAF) from AMBER (v3.9),[53] read depth ratios from COBALT (v1.13),[53] somatic SVs from GRIDSS and GRIPSS, and somatic and germline short variants from SAGE and PAVE to estimate variant allele frequency (VAF) and DNA copy number profiles. LINX (v1.19)[55] was used to chain, classify, and visualize somatic SVs from PURPLE.

To compare the VAF distribution of somatic short variants between tumor tissue and tumor organoid from the same patient, SAGE and PAVE were used to annotate somatic short variants (SNVs, MNVs and INDELs) in multiple tumor samples module, adjacent normal tissue was input as reference sample, tumor tissue and tumor organoid were both input as tumor sample. For SNV overlap analysis high confidence somatic mutations were retained that (a) had a minimum of 20 reads present across tumor, organoid and adjacent normal tissue at the SNV location, and (b) had an alternate allele frequency of at least 20% in at least one of the tumor tissue or tumor organoid samples.

RAS, *RAF* mutation and DNA mismatch repair status

RAS (*KRAS*, *NRAS*; exons 2, 3 and 4 in both genes) and *RAF* (*BRAF*^{V600E}) mutation status were assessed by routine clinical sequencing assays as per Australian Medicare Benefits Schedule Item 73338. Tumor DNA mismatch repair status was determined based on standard diagnostic assays for mismatch repair proteins (MLH1, MSH2, PMS2 and MSH6) or the Bethesda consensus panel of microsatellite markers (BAT25, BAT26, D2S123, D5S346, and D17S250).[62,63] For IHC, mismatch repair-deficient was defined as absence of nuclear staining in tumor cells but positive nuclear staining in stromal cells and lymphocytes for at least one mismatch repair protein. For the Bethesda consensus panel, mismatch repair-deficient status was diagnosed if instability was detected at two or more markers.

Semiautomated PDTO drug assay

PDTO drug profiling was performed on a previously validated, standardized drug testing platform in 384-well format with seeding of 2,000 to 3,000 single cells per well using a MANTIS Microfluidic Liquid Dispenser (Formulatrix, 0695).[25] PDTOs were collected at 200 g for 3 min, washed with PBS at 200 g for 3 min, digested with TrypLE Express enzyme (Thermo Fisher Scientific, 12604021) at 37°C for 10 min, washed with DMEM/F12 at 200 g for 3 min, resuspended in PDTO LVM culture medium culture medium, and then dissociated with 26G needles and filtered through 70-μm cell strainers (Bio-Strategy, FAL 352350) to produce a single-cell suspension. Single cells were then suspended in PDTO LVM culture medium with the addition of 1x penicillin-streptomycin (Life Technologies, 15140122), 100 μg/mL normocin (Invivogen, ant-nr-2), 10 μM Y27632 and 3% Matrigel, seeded into 384-well plates (Thermo Fisher Scientific, 242764) and cultured for 3 days at 37°C in 5% CO_2 before drug treatment. Using a JANUS Liquid Handler Workstation (PerkinElmer) with PinTool addition accessory (PerkinElmer), single agents were assayed in duplicate in 9 point, 4-fold dilution series with starting concentrations of 50 μM for 5-fluorouracil, 75 μM for oxaliplatin, 0.5 μM for SN38, 50 μM for regorafenib, 50 μM for TAS-102, 15 μM for gemcitabine, 10 μM for pemetrexed, 750 μM for temozolomide and 50 μM for erlotinib. FOLFOX and FOLFIRI treatments were assayed in duplicate in 7x7 drug matrices with 4-fold dilution series with starting concentrations of 50 μM for 5-fluorouracil, 75 μM for oxaliplatin and 0.5 μM for SN38 treatment components. DMSO 0.5% (v/v) and 1 μM bortezomib served as negative (vehicle) and positive (killing) controls, respectively. PDTO cultures were imaged daily for 7 days by bright-field microscopy on an automated Nikon Eclipse Ti2 Inverted Microscope System (NIS-Elements AR software version 5.21.03, 64-bit)

with a 4× objective and a 25 μm z stack over a 500 μm range. Image analysis to determine PDTO sizes was performed using ImageJ software (NIH Image).[56] PDTO viability normalized to negative and positive controls was calculated as (Mean PDTO $size_{Treatment}$ - Mean PDTO $size_{Killing\ Control}$)/(Mean PDTO $size_{Vehicle\ Control}$ - Mean PDTO $size_{Killing\ Control}$). Dose-response curves were fitted to determine effective concentration metrics (EC). *In vitro* responses were quantified as area under the drug response curve (AUC) for single agents and mean 'pan-matrix' viability score for drug combinations. For drug response measurements using the window design, the average of the respective PDTO viability scores was calculated.

QUANTIFICATION AND STATISTICAL ANALYSIS

Study data were collected and managed using REDCap electronic data capture tools hosted by the Clinical Translation Center at WEHI.[64] Statistical analyses were performed using the statistical computing software R (version 4.2.0).[57] Specific analysis methods for each datasets are specified in the figure and table legends. Differences between groups were assessed using the Fisher's exact test for categorical variables and the Student's *t* test for continuous variables. Correlations between continuous variables were assessed using Pearson correlation coefficient and correlation test. Assay prediction accuracy as compared to non-informative rate was assessed using the binomial test. Data were presented as Mean ± standard deviation in bar charts. Progression-free survival (PFS) was defined as the time from treatment start date to clinician assessed disease progression with censoring done when a patient died or was alive without disease progression at last contact. Associations between PDTO drug predictions and PFS were assessed using Kaplan Meier survival curves and the log rank test; hazard ratios and 95% confidence intervals were calculated using Cox proportional hazard models. All statistical analyses were two-sided and considered significant if $p < 0.050$.

ADDITIONAL RESOURCES

- AGITG FORECAST-1 was a prospective, observational clinical study comprising 30 patients with mCRC who had failed ≥ two lines of therapy (Clinical Trial Registration Number: ACTRN12620001353987).
- Link to AGITG FORECAST-1 study: https://gicancer.org.au/clinical-trial/forecast-1/.